The Pennsylvania State University
APPLIED RESEARCH LABORATORY
Post Office Box 30
State College, PA 16804

Experimental Measurements of the Demo Enclosure

by

J. B. Fahnline, R. L. Campbell, and S. A. Hambric

Technical Report 04-006
May 2004

E. G. Liszka, Director
Applied Research Laboratory

REPORT DOCUMENTATION PAGE	Form Approved OMB No. 0704-0188

1. REPORT DATE *(DD-MM-YYYY)*	2. REPORT TYPE	3. DATES COVERED *(From - To)*
May 2004	Technical Report	

4. TITLE AND SUBTITLE

Experimental Measurements of the Demo Enclosure

5a. CONTRACT NUMBER

PL01000100

5b. GRANT NUMBER

5c. PROGRAM ELEMENT NUMBER

6. AUTHOR(S)

J. B. Fahnline, R. L. Campbell, and S. A. Hambric

5d. PROJECT NUMBER

5e. TASK NUMBER

5f. WORK UNIT NUMBER

7. PERFORMING ORGANIZATION NAME(S) AND ADDRESS(ES)

Applied Research Laboratory
Post Office Box 30
State College, PA 16804

8. PERFORMING ORGANIZATION REPORT NUMBER

TR 04-006

9. SPONSORING/MONITORING AGENCY NAME(S) AND ADDRESS(ES)

10. SPONSOR/MONITOR'S ACRONYM(S)

11. SPONSOR/MONITOR'S REPORT NUMBER(S)

12. DISTRIBUTION/AVAILABILITY STATEMENT

Approved for public release. Distribution unlimited

13. SUPPLEMENTARY NOTES

14. ABSTRACT

Surface vibrations and sound radiation from a small enclosure, meant to simulate the basic characteristics of an equipment enclosure but without the complexity, are investigated experimentally. Several methods of mounting interior shelves in an enclosure are tested, with an attempt to simulate free-free, simply-supported, and clamped boundary conditions. As expected, the measurements show that the vibrations and sound radiation are intimately related to the way the shelves are mounted in the enclosed. Overall, the demo enclosure measurements have yielded valuable information about the effects of the shelf boundary conditions on noise radiation.

15. SUBJECT TERMS

16. SECURITY CLASSIFICATION OF:			17. LIMITATION OF ABSTRACT	18. NUMBER OF PAGES	19a. NAME OF RESPONSIBLE PERSON
a. REPORT	b. ABSTRACT	c. THIS PAGE			19b. TELEPHONE NUMBER *(Include area code)*
Unclassified	Unclassified	Unclassified	Unclassified Unlimited-UU	46	

Standard Form 298 (Rev. 8/98)
Prescribed by ANSI Std. Z39.18

TABLE OF CONTENTS

Page Number

LIST OF FIGURES

LIST OF FIGURES (CONT'D)

LIST OF FIGURES (CONT'D)

INTRODUCTION

The "demo enclosure" is a small box constructed at ARL/PSU to simulate the basic characteristics of an equipment enclosure, but without the complexity of an actual enclosure. In the general case, an equipment enclosure can house a variety of electrical equipment, including transformers, card racks, etc., usually mounted on shelves. We are primarily interested in investigating the best way to mount the shelves in the enclosure to mitigate sound radiation due to the excitation from the electrical equipment. A secondary goal is to assess methods for modeling the structural properties of interconnected shelves and cabinets along with the electrical equipment. In this report, we will concentrate on the extensive experimental measurements made during the investigation.

A. Demo Enclosure Specifications

To keep the cost of making the demo enclosure reasonable, it was fabricated from readily available pieces of stock aluminum screwed together with 1/4 " steel screws. Figure 1 shows a picture of the actual enclosure and a one quarter finite element model, which in the context of this report is used primarily to help identify the various parts. The enclosure was fabricated by first connecting the four side walls together with vertical angles. The same type of angle is used for all of the parts with 1 1/4 " legs and 3/16 " thickness, as shown in Figure 2. The angles and plates are screwed together at approximately 2 " intervals along the 24 " height. The plating for all the walls, including the top and bottom surfaces, is 3/32 " thick. The next step in the fabrication was to reinforce the top and bottom plates by adding angles along the edges. The ends of the angles are cut at 45 degrees so that they mate at the corners, but are not actually physically joined to each other. The top and bottom surfaces are precisely 19 3/16 " x 24 3/16 " and fit snugly into the opening at the top and bottom of the enclosure. After the bottom is mounted in the enclosure, the shelf is inserted with its top surface at a height of 12". The shelf is twice the thickness of the plating used for the walls, and is also reinforced with angles. Its outer dimensions are slightly smaller that those for the top and bottom surfaces, such that there is a 1/16 " gap around its perimeter when it is placed inside the enclosure. Finally, after the shelf is in place, the top surface is mounted.

Three different connections between the shelf and the enclosure walls were tested. In the first configuration, one inch aluminum cubes were attached inside the enclosure as supports of the shelf at its corners. To help to isolate the shelf from the walls, a 1/4 " thick layer of the isolation material sorbothane was placed on top of each of the cubes. The shelf then rested on top of the sorbothane. In the second configuration, hinges were used to connect the top surface of the shelf to the enclosure walls. In theory, the hinges should allow the shelf and the walls to rotate independently along the hinge axis. In the third configuration, referred to as "clamped", 1/16 " shims were placed around the shelf and it was rigidly attached to the walls with screws. The bare shelf was also tested without any equipment, with "dummy masses", and with real equipment (which was meant to duplicate the complexity of actual electrical equipment without being functional). The dummy masses were fabricated to simulate the masses and inertias of the real equipment. Figure 3 shows the dummy masses and real equipment mounted to the plate.

B. Experimental Measurement Suite

For each configuration, two separate tests were performed. In the first test, a roving force hammer was used to measure transfer functions between input normal force and acceleration at 15 fixed locations simultaneously. Figure 4 shows the hammer impact locations on the outside of the enclosure. Two accelerometers were placed on each of the walls, including the top and bottom, and three were placed on the shelf. The accelerometers were placed near corners, away from symmetry axes, so that they did not intersect nodal lines. The data from the test was used to perform modal analyses using the singular value decomposition (SVD), and, in conjunction with the acoustic boundary element program POWER [1], was used to compute radiated noise for drive point locations on the shelf. The closed surface mesh in Figure 4 was used for the boundary element analysis.

In the second test, two small electromechanical shakers were mounted to the underside of the shelf coincident with accelerometer locations, as shown in Figure 5, and sound pressure levels were measured at various points surrounding the enclosure with one of the shakers activated. Transfer functions were also measured for the accelerometer locations on the outer walls and the shelf. The data from this test was used as an ultimate measure of the radiated noise for each of the shelf boundary conditions. Since the shelf is not accessible when the enclosure is fully assembled, it also provided some limited transfer function data for drive and response points both located on the shelf.

C. Modal Analysis Using the Singular Value Decomposition

Experimental modal analyses were performed for nine configurations: (1) bare shelf alone on bubblewrap, (2) bare shelf resting on sorbothane on the ground, (3) bare shelf resting on sorbothane in the enclosure, (4) enclosure without the shelf, (5) enclosure with the bare shelf resting on sorbothane, (6) enclosure with the bare shelf hinged, (7) enclosure with the bare shelf clamped, (8) enclosure with the shelf clamped with dummy masses, and (9) enclosure with the shelf clamped with real equipment. Rather than trying to present all of the modal data, we will compare and contrast their basic characteristics for the different configurations.

Bare shelf alone. We will begin with the three sets of data for the bare shelf alone. For the test with the shelf resting on sorbothane in the enclosure, the top plate of the enclosure is removed to allow access into the interior. Figure 6 shows the integrated squared normal velocity over the surface of the shelf for each configuration. Clearly, the damping levels increase dramatically when the shelf is resting on sorbothane, which is confirmed by the loss factor plot in Figure 7. The increased loss factor for the shelf in the enclosure in comparison to the shelf on the ground indicates that some of the energy is being transferred to, and dissipated in, the enclosure walls. The first three modes for each configuration are shown in Figure 8. The lowest order mode is somewhat effected by the boundary conditions for the shelf, but otherwise there is little difference. The test with the shelf resting on sorbothane on the ground was performed to confirm that the sorbothane was the primary cause of the unexpectedly high damping levels. The results for the shelf resting on sorbothane were somewhat of a surprise because our original intent was to

reproduce free-free boundary conditions, which should have produced damping levels comparable to those for the shelf resting on bubble wrap.

Enclosure with the shelf resting on sorbothane. When the shelf is in the enclosure resting on sorbothane, the modes of the enclosure walls are very similar to those without the shelf. To demonstrate, Figure 9 shows the first four modes for both configurations. Only a coarse grid of experimental data was taken for the enclosure without the shelf because it was used only to compare to the other configurations. Despite the differences in mesh resolution, it is clear from the results that the modes change little when the shelf is resting on sorbothane. Similarly, Figure 10 shows a comparison of the vibration levels for the two configurations with the drive and response points both located on Side A, the location of which was illustrated previously in Figure 4. Clearly, the presence of the shelf does not significantly change the response of the shelf walls.

We also recall from the previous section that the vibrations of the shelf itself do not change significantly whether it is mounted in the enclosure or sitting on the ground. Further confirmation of the nature of the shelf vibrations was obtained from the second set of tests using the shaker as an excitation source. Figure 11 shows the acceleration at a point on the shelf for a drive point on the shelf, the modal content of which can be compared to that shown previously in Figure 6. For the configuration with the shelf resting on sorbothane, the combined enclosure - shelf system is thus essentially the summed response of the two independent components, with relatively small coupling.

The main difference between the enclosure with no shelf and with the shelf resting on sorbothane is an increase in the loss factor, as illustrated in Figure 12. Surprisingly, the damping increases significantly even for the low frequency modes below 100 Hz which are dominated by vibrations of the enclosure walls. It would be interesting to know if the damping levels would decrease back to their original levels if the shelf is more securely fastened at the corners rather than simply resting on sorbothane, but this configuration was not tested.

Enclosure with the shelf hinged to the sides. When the shelf is hinged to the enclosure walls, we expect to see an increase in the coupling between the shelf and the walls and an overall increase in the stiffness and resonance frequencies. Figure 13 shows the first eight modes of the enclosure with the shelf hinged to the walls. We note that the hinges enforce a nodal line in the plane of the shelf, such that it acts like a stiffener for the sidewalls. Figure 14 shows a comparison between the integrated normal velocity over the enclosure walls for a drive point on the shelf (off-center, such that most of the modes should be excited) with the shelf resting on sorbothane and hinged to the sides. The results show that the coupling between the shelf and wall vibration is considerably larger when the shelf is hinged, giving much higher vibration levels. This contrasts with a drive point on the wall, which results in only slight differences between the two configurations. Figure 15 shows the loss factor comparison with the shelf resting on sorbothane and hinged to the sides, and, again, there are only slight differences between the two configurations. The level of coupling between the shelf and the enclosure walls can be assessed in a relative sense by comparing the measured acceleration levels for various locations, as shown in Figure 16, where heavily-coupled modes are marked with an arrow. The results show that the shelf is now fully-coupled to the walls of the enclosure and the two systems cannot be considered as being independent with small coupling.

Enclosure with the shelf clamped to the sides. When the shelf is clamped to the enclosure walls, we expect further increases in the overall stiffness level and in the coupling between the shelf and the walls. Figure 17 shows the first eight modes of the enclosure with the shelf clamped to the walls. In comparison to the mode shapes for the hinged configuration, there is now a much greater tendency for the top or bottom halves of the side walls to vibrate independently of each other. Figure 18 shows a comparison between the integrated normal velocity over the enclosure walls with the shelf hinged and clamped to the sides. The overall levels are similar except in the range between 150 and 250 Hz, where they are significantly higher for the clamped shelf. Figure 19 shows the loss factor comparison with the shelf hinged and clamped to the sides, and there is possibly a slight decrease in the loss factors for the clamped configuration. As a side note, the vibration levels of the enclosure walls are not significantly changed by the boundary conditions for the shelf. To illustrate, Figure 20 shows the integrated squared normal velocity over the enclosure walls for a drive point on Side A. Although there are some shifts in the resonance frequencies due to the stiffening effects of the shelf, the overall levels do not change significantly.

Enclosure with the shelf clamped and with dummy masses. When the dummy masses are added, we expect the modes involving the shelf to shift downward in frequency. Figure 21 shows the first eight modes of the enclosure with the shelf clamped to the walls and with added dummy masses. The main obvious difference is in mode number three, whose resonance frequency is reduced from 109.93 Hz in Figure 17 down to 97.14 Hz. The remaining modes do not shift significantly, leading to the conclusion that they are not highly coupled to the shelf vibration. Figure 22 shows a comparison between the integrated normal velocity over the enclosure walls with the shelf clamped and with it clamped with added dummy masses. The overall levels are similar except near shelf resonances, where the vibration response of the walls of the enclosure is reduced considerably when the dummy masses are added. Figure 23 shows the loss factor comparison between the bare clamped shelf and the clamped shelf with added dummy masses. Overall, the addition of the dummy masses yields slightly larger loss factors, but not uniformly.

Enclosure with the shelf clamped and with real equipment. When real equipment is added to the shelf, some of the resonances should again shift downward. We also expect increased damping loss factors because energy will be transferred to the equipment itself where it will be dissipated. Figure 24 shows the first eight modes of the enclosure with the shelf clamped to the walls and with real equipment added. As for the configuration with the added dummy masses, the main difference is in the third mode, whose resonance frequency is considerably reduced in comparison to the bare shelf configuration. Figure 25 shows a comparison between the integrated normal velocity over the enclosure walls with the shelf clamped with added dummy masses and with it clamped with real equipment. We recall that the dummy masses are meant to simulate the basic structural properties of the real equipment as they might be modeled in a simplified finite element analysis. The test results were to serve as a "proof of concept". Overall, there is relatively little difference in the vibration response of the enclosure walls for the two configurations. Figure 26 shows the loss factor comparison with the shelf clamped with added dummy masses and with it clamped with real equipment. As expected, there is a slight increase in the damping loss factor with the real equipment added to the shelf, but the increase is not uniform as a function of frequency. Also, the configuration with real equipment shows a slight increase in the modal density in comparison to that for the dummy masses. Finally, Figure 27 shows a comparison of the

drive point accelerance for the three configurations with the shelf clamped to the enclosure walls. Clearly, adding the dummy masses or real equipment considerably reduces the vibration levels.

D. Pressure Measurements and Predictions

For the second test, the shelf was driven with a shaker and sound pressure levels were measured at ten locations near the outer surface of the enclosure, as illustrated by the small colored squares in Figure 28, and at a single location in the interior. The measured pressures were compared to predictions from the boundary element program POWER using the measured vibration data from the hammer test as input. Because the shakers were not mounted in the enclosure during the hammer test, the resonance frequencies do not line up exactly between the data from the hammer and shaker tests, but the computed pressures should still compare fairly well with the experimental measurements. We will not show any of the data for the interior pressures in this report because it cannot be predicted using our computational procedure without data for the vibrations of the shelf.

Measurements and predictions were made for the five configurations with the shelf inside the enclosure. Rather than trying to compare the pressure spectra at each of the individual microphone locations, the data was power-summed and converted to an approximate radiated acoustic power output, which could then be compared to the numerical power output predictions. In general, the power-summed pressures will include contributions from modes that radiate sound inefficiently and thus would not be measurable in the farfield. However, we can check how well the power-summed pressures approximate the radiated power output by comparing the two quantities for the numerical computations. Figures 29 though 33 show the predicted power output along with power-summed pressures derived from the experimental measurements and numerical computations. Overall, the numerical predictions correspond well to the experimental measurements, especially considering the differences in the two testing configurations. As an example, in Figures 30 and 31 the downward shift in the resonance at approximately 110 Hz due to the added mass of the shaker is clearly evident in the measured pressures. The shift is also present in Figures 32 and 33, but the mass of the shaker does not cause nearly as large of a deviation because the shelf is so much heavier once the attachments have been added. Finally, Figure 34 shows a comparison between the computed power output and the corresponding monopole approximation for the configuration with real attachments mounted on the clamped shelf. In general, the calculation of the monopole approximation is fast because it can be computed directly from the surface displacements without a boundary element analysis. The results show reasonable agreement, but because the number of elements in the boundary element model is small, there is really no reason not to perform the full analysis and obtain more accurate predictions. This guidance may be more valuable for fully numerical calculations where the boundary element meshes are much more dense and the computation times are much longer.

We now have enough data to assess the effect of the boundary conditions for the shelf on the radiated noise from the enclosure. Comparing Figures 29-33, we can draw the general conclusion that the radiated noise is mitigated by connecting the shelf to the enclosure walls as softly as possible. Although this result was expected, it is still useful because we now have a quantitative assessment of the range of the radiated noise spectrum for various boundary conditions. Obviously, there are limits to how softly the shelf can be connected to the enclosure

because it must be able to withstand a certain amount of shock loading. However, this still leaves a wide range of possible mounting configurations to be explored.

CONCLUSIONS

Overall, the demo enclosure measurements have yielded valuable information about the effects of the shelf boundary conditions on noise radiation. As might be expected, reducing the coupling between the shelf and the enclosure walls was demonstrated to reduce the radiated noise. In a practical application, the shelf should only be connected to the enclosure at its corners and should be soft mounted. Even though this will undoubtedly result in increased vibration levels of the shelf, it should not preclude a practical design that will withstand shock loading.

A second conclusion from the analysis is that the boundary element program POWER gives reasonable predictions of the radiated noise using the measured surface vibrations as input for the normal velocity boundary condition. It has also been shown that once the surface vibrations are known, it is possible to compute a reasonably accurate prediction for the radiated noise using a simple monopole approximation. Unfortunately, these types of analysis may not be practical for enclosures with considerably larger dimensions because of the required number of measurement locations.

For our secondary goal of comparing the enclosure response with real equipment or dummy masses mounted to the shelf, the results show that using the dummy masses leads to a reasonably accurate simulation of the overall radiated noise with the real equipment attached, but does not necessarily yield accurate information for the resonance frequencies of the offending modes or the precise radiated noise levels. Presently, it is unknown whether the differences are primarily due to differences in the structural properties of the dummy masses or in the mounting conditions.

Finally, the measurements have provided a detailed database of experimental configurations to use in verifying accompanying finite and boundary element models. Because of the large amount of data, we have made an effort to distill the results down as much as possible while still providing useful information. This is especially true of the modal analysis data for the enclosure because the original datasets are extremely large. Despite the amount of data, all the analysis programs ran flawlessly on PC's with approximately 1Gb of RAM. All of the data has been archived and is available for further study.

REFERENCES

The authors would like to express their gratitude to Wayne J. Holmberg and Greg E. Seeger for performing the extensive experimental measurements described in this report. Without their efforts, this research would not have been possible.

REFERENCES

[1] G. H. Koopmann and J. B. Fahnline, *Designing Quiet Structures: A Sound Power Minimization Approach*, (Academic Press, New York, 1997).

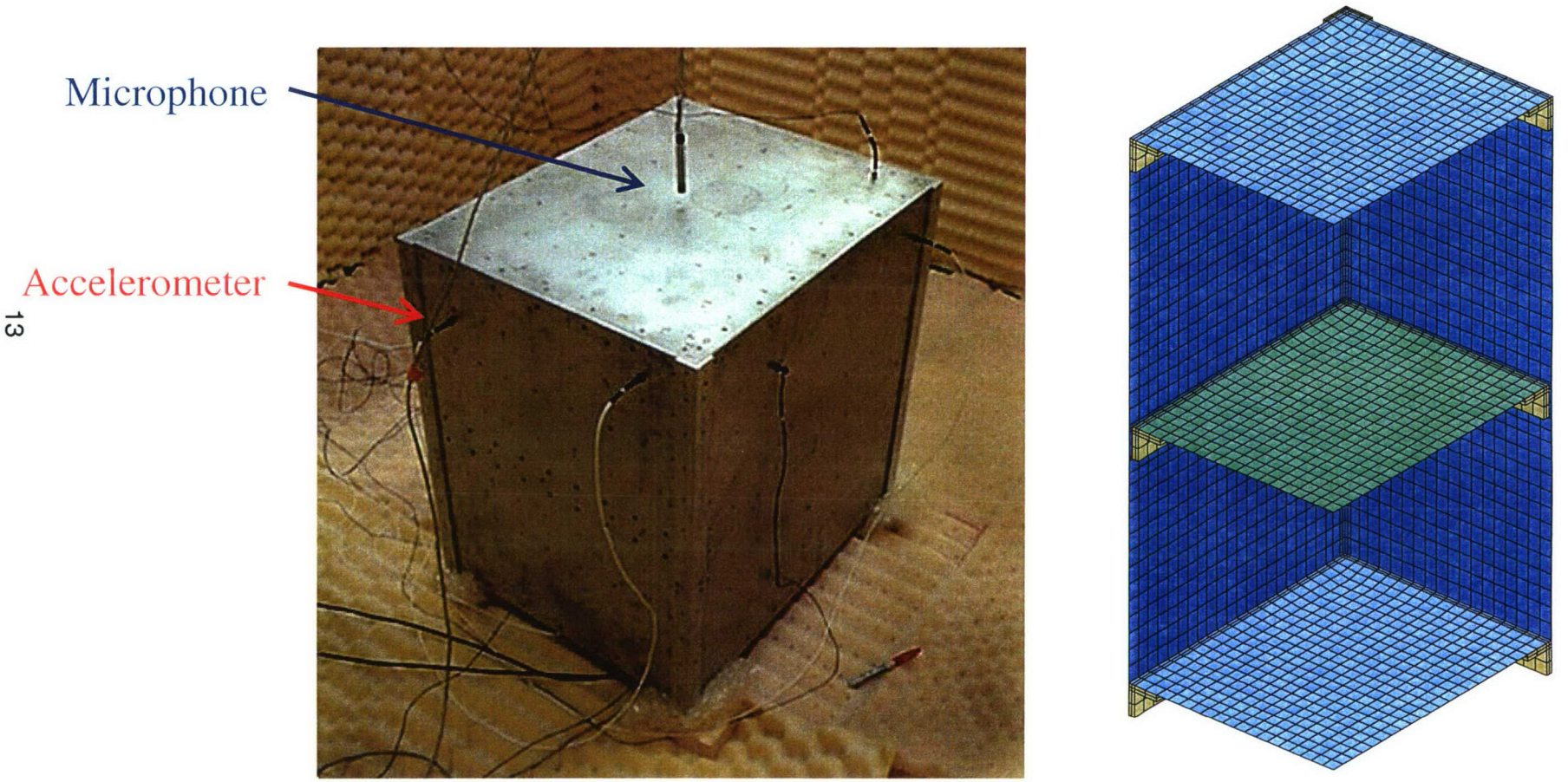

Figure 1. Photograph and ¼ finite element model of the demonstration enclosure

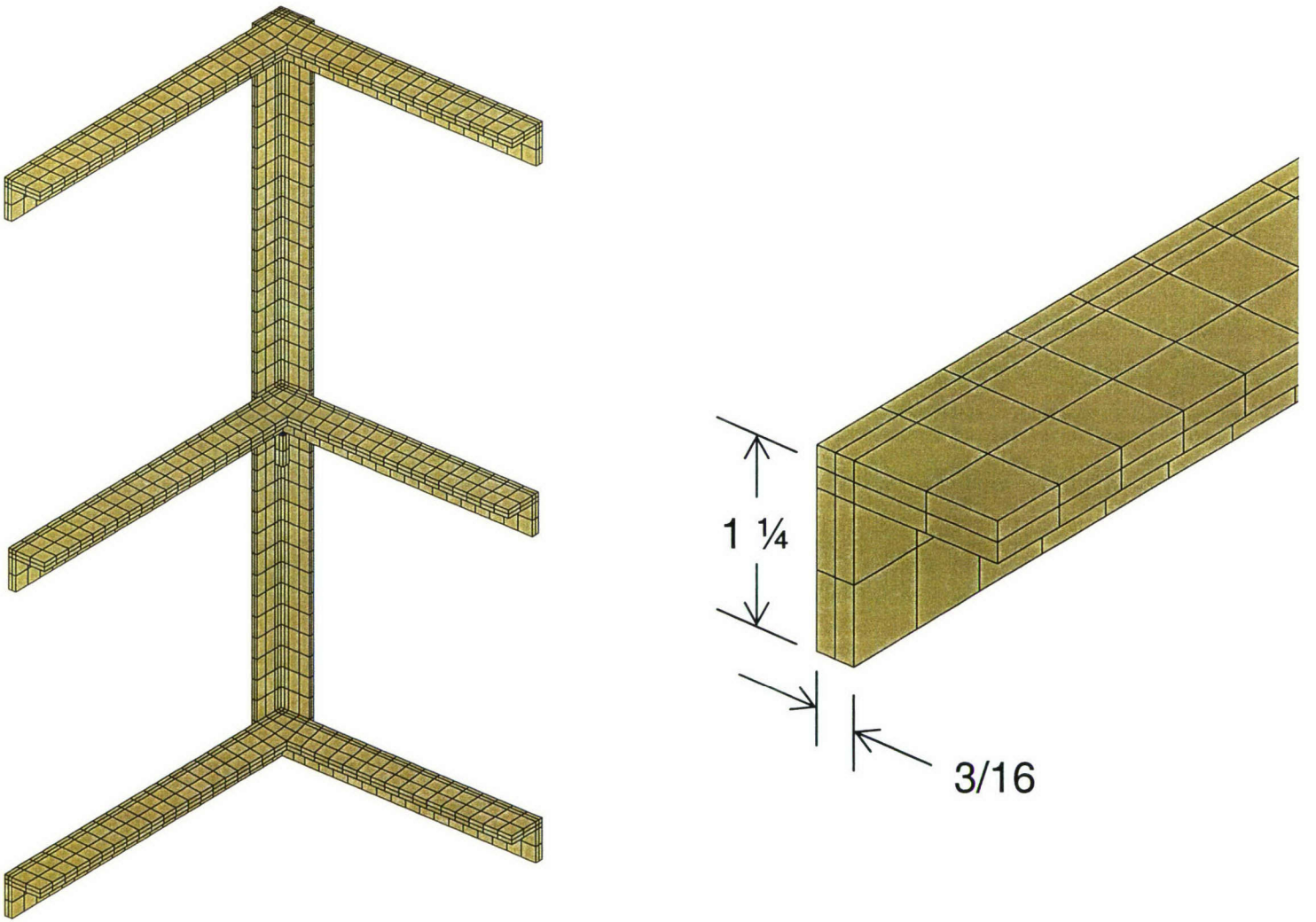

Figure 2. Illustration of the frame and the dimensions of the angles

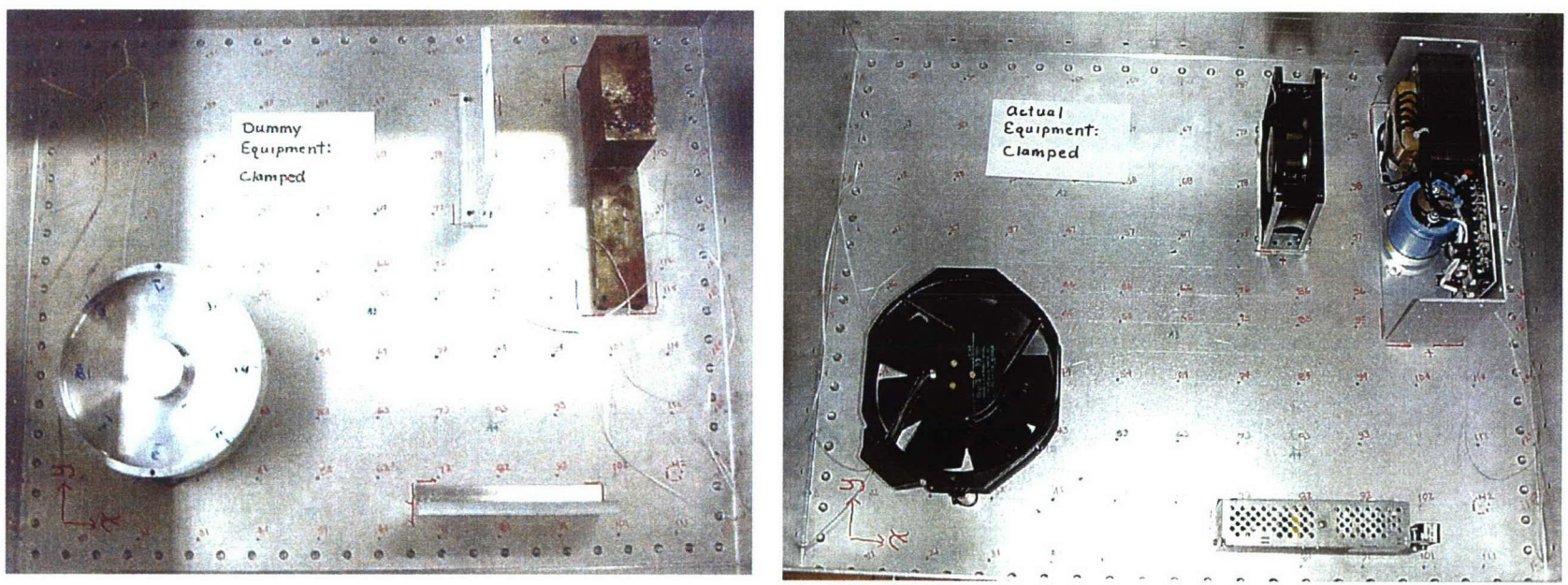

Figure 3. Photographs of the shelf with dummy masses and with real equipment

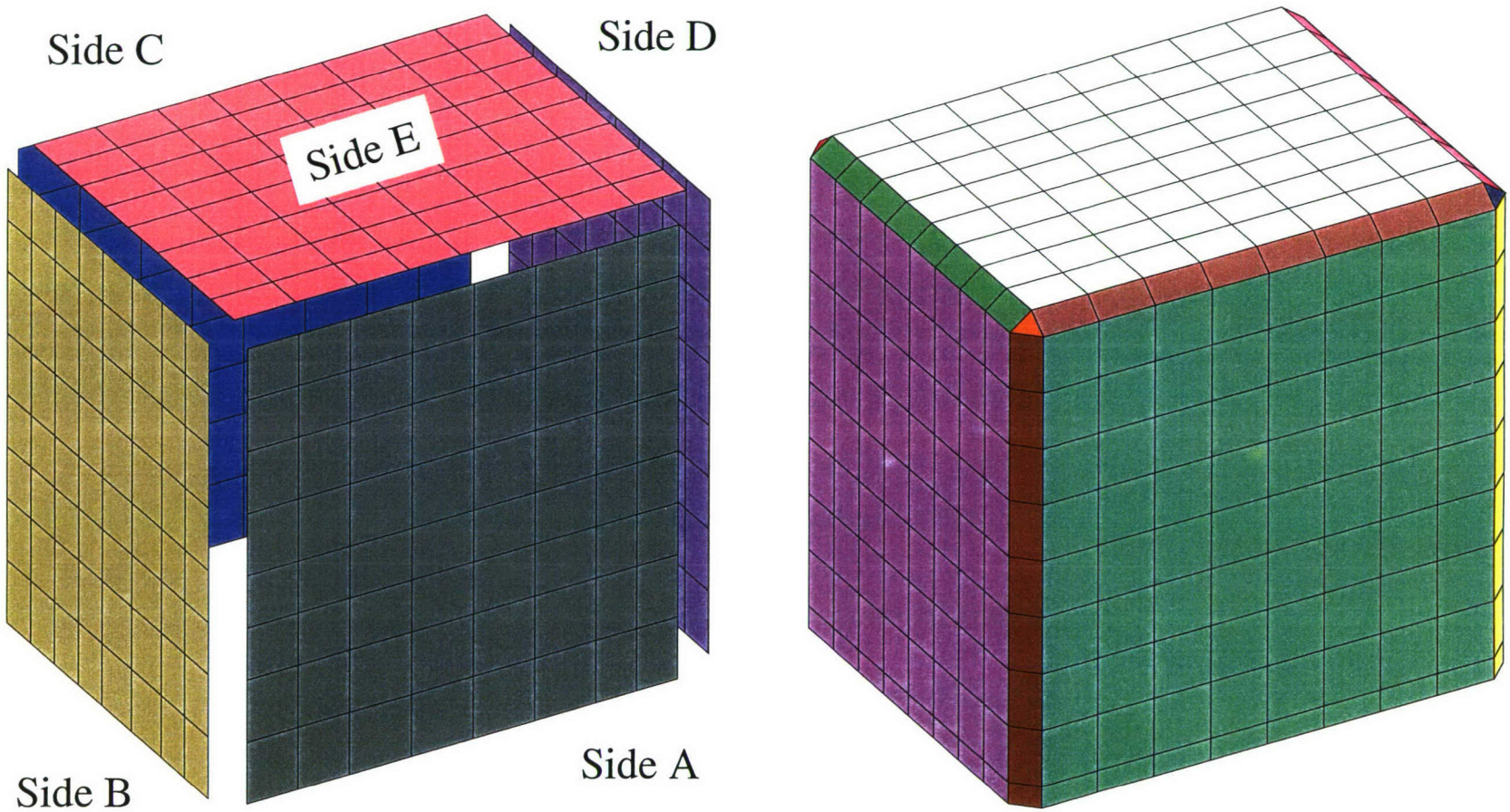

Figure 4. Measurement grid for the enclosure and the resulting boundary element mesh

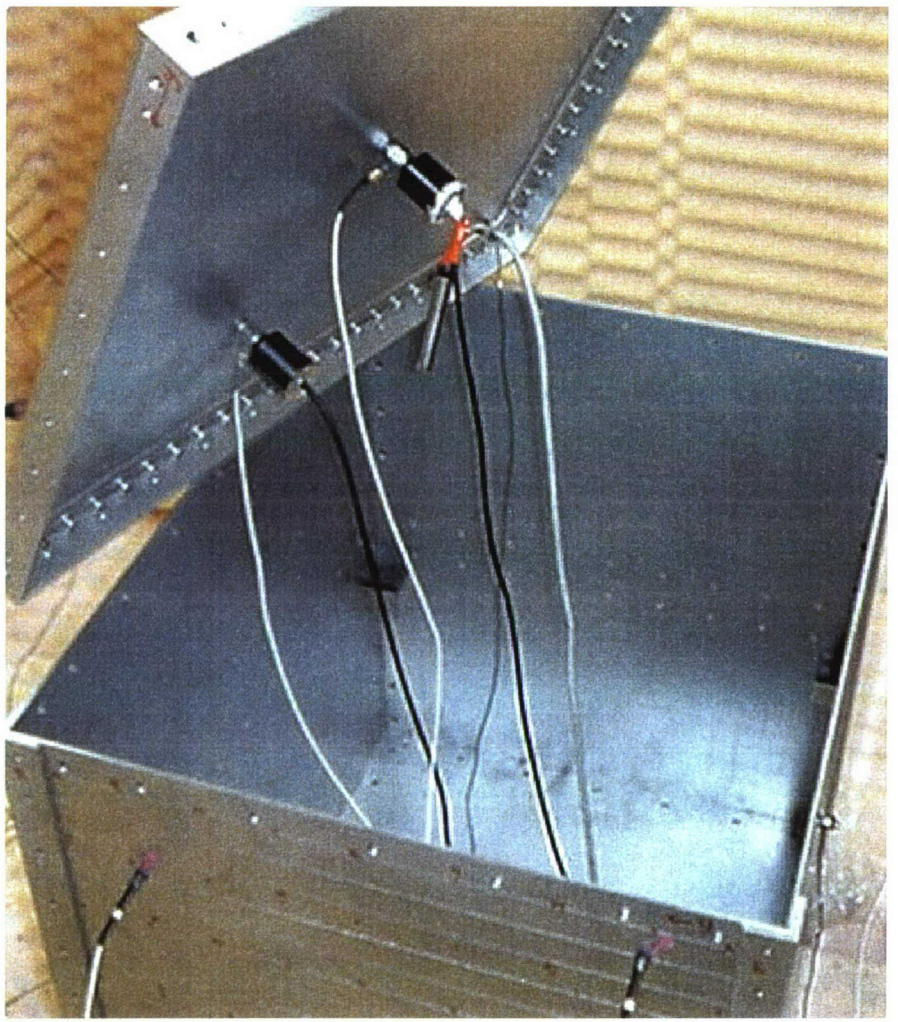

Figure 5. Photograph of the shelf showing the shakers mounted on its underside

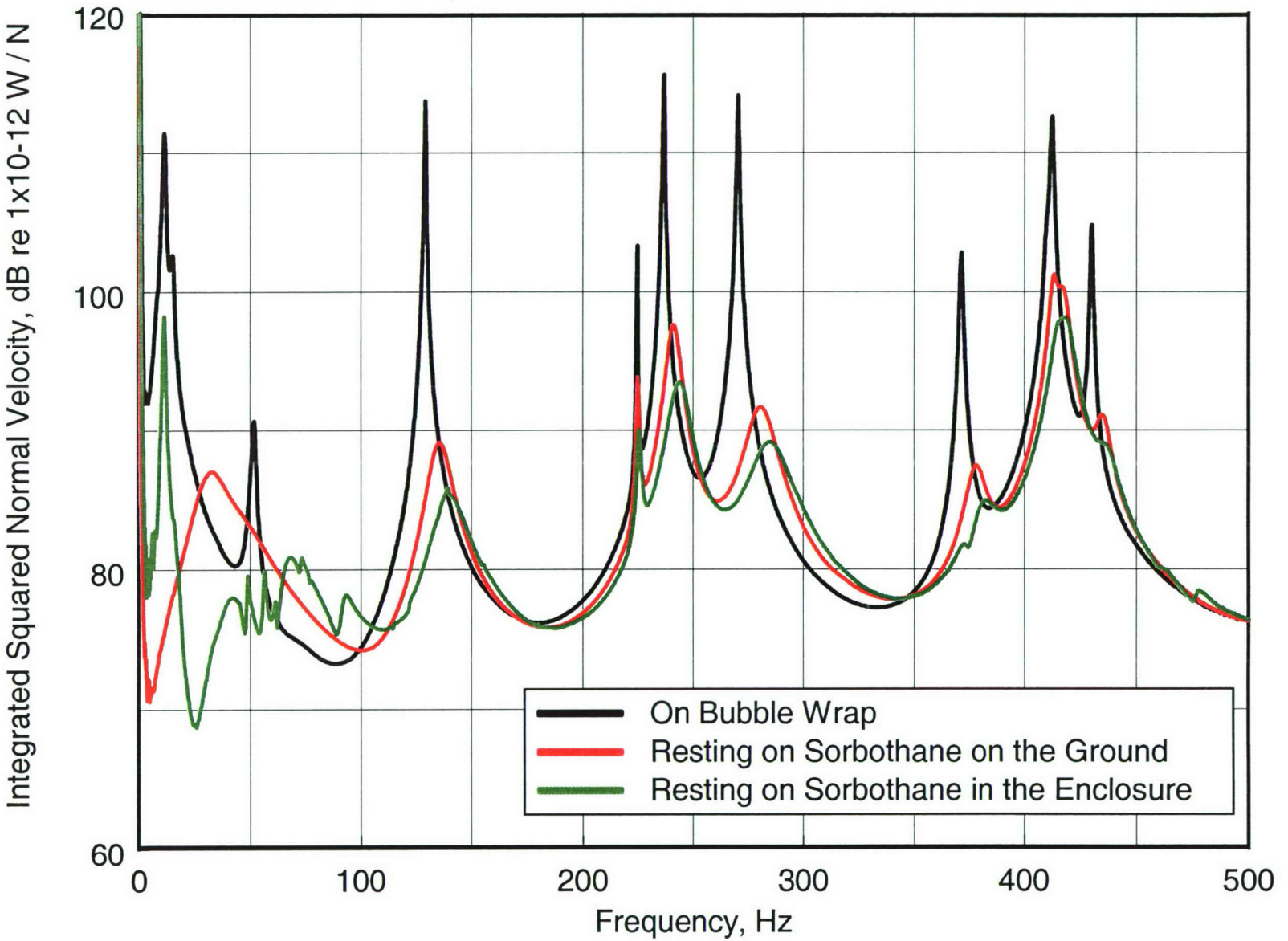

Figure 6. Comparison of the vibration levels for the shelf with various boundary conditions

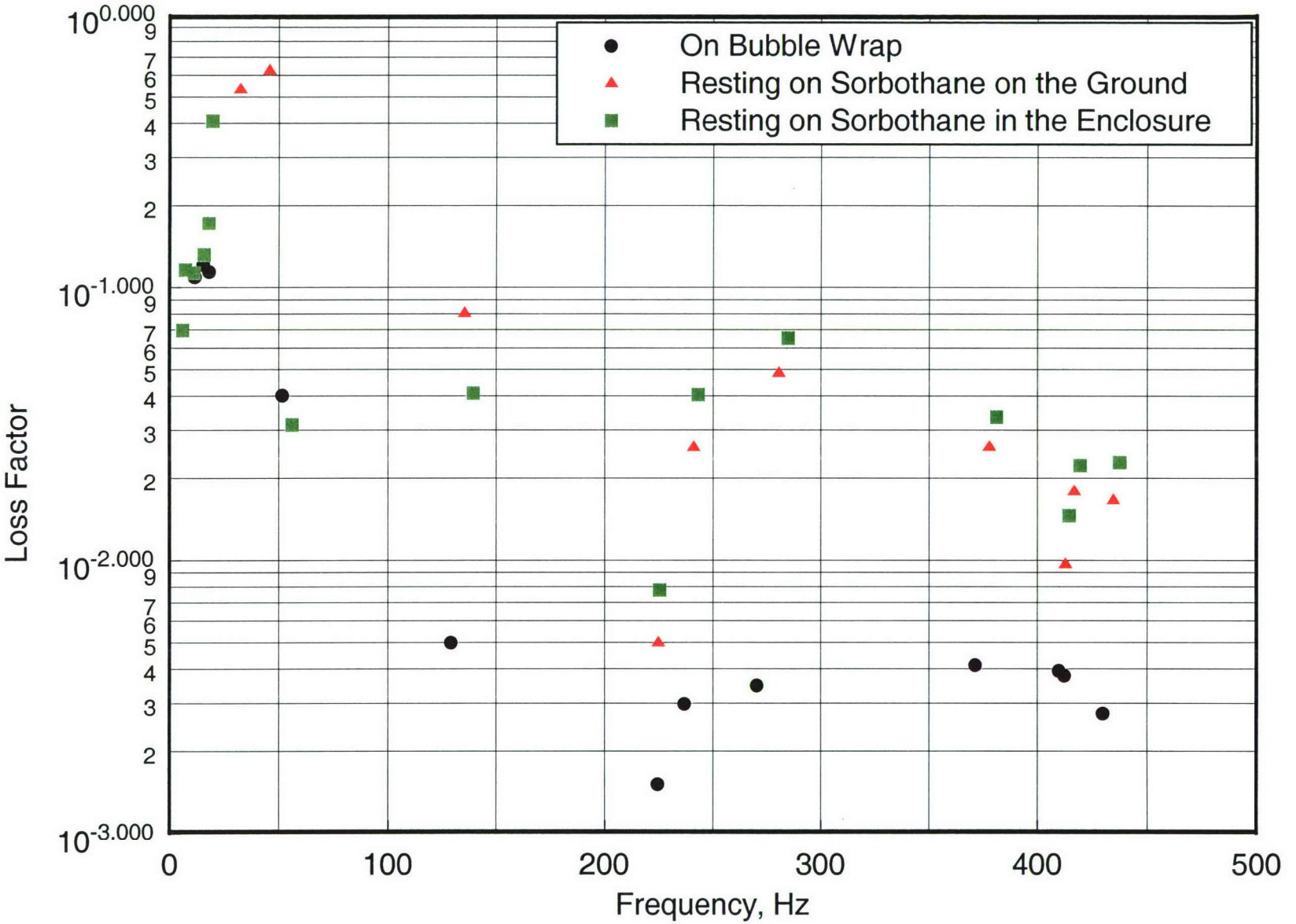

Figure 7. Comparison of the damping loss factors for the shelf with various boundary conditions

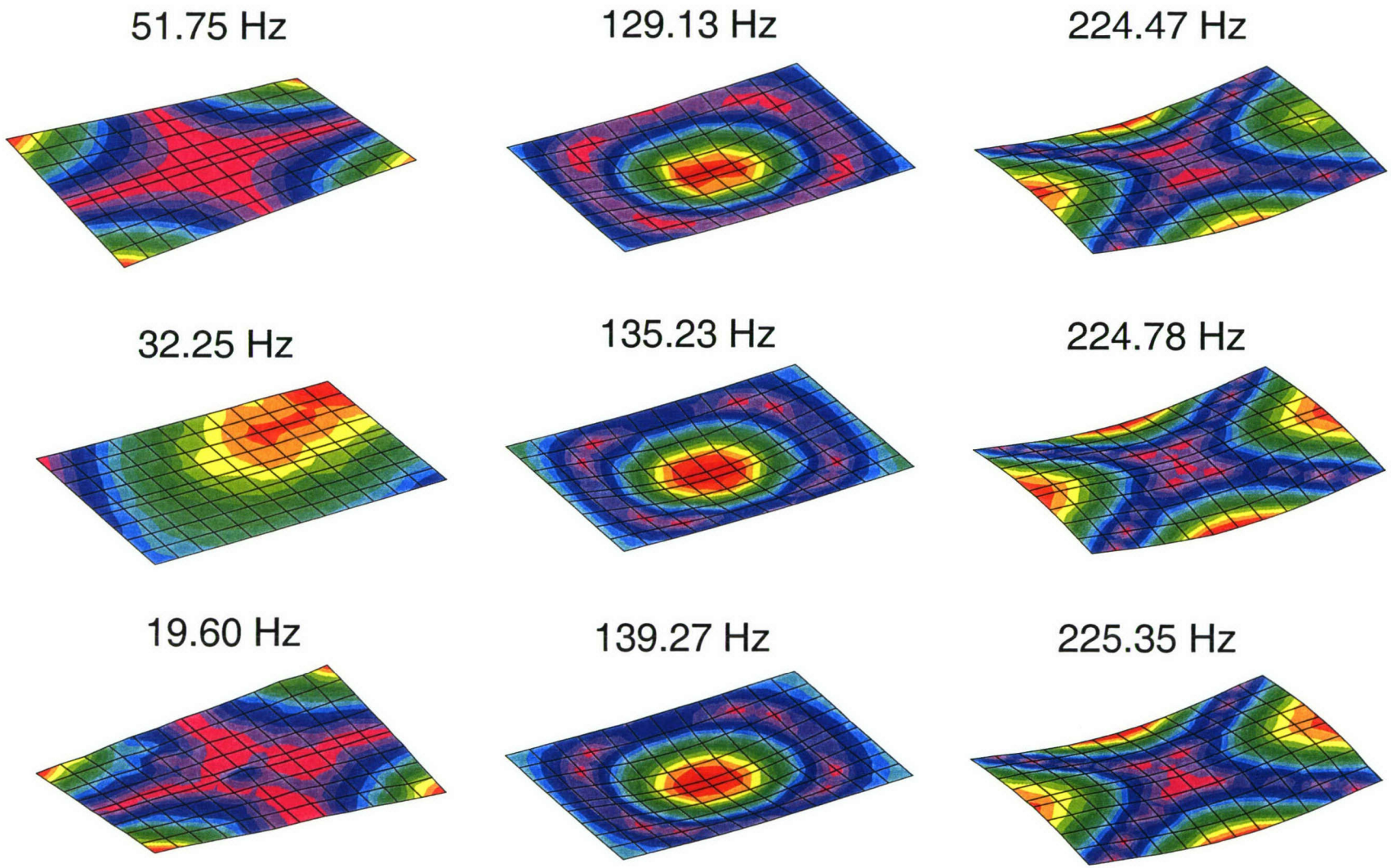

Figure 8. Mode shape comparison for the bare shelf (top - on bubble wrap, middle - on the ground resting on sorbothane, bottom - in the enclosure resting on sorbothane)

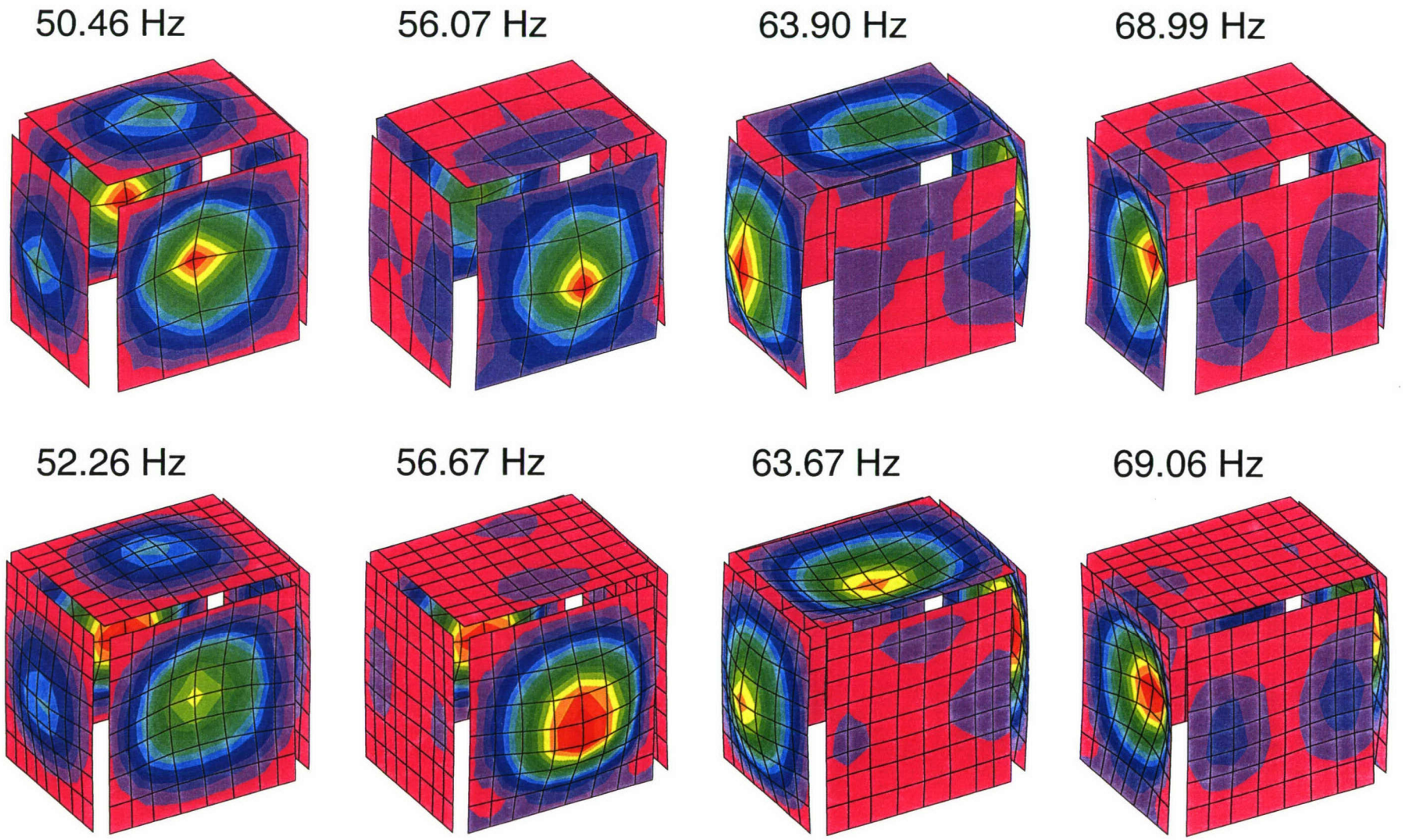

Figure 9. Mode shape comparison for the enclosure (top – without shelf, bottom – shelf resting on sorbothane)

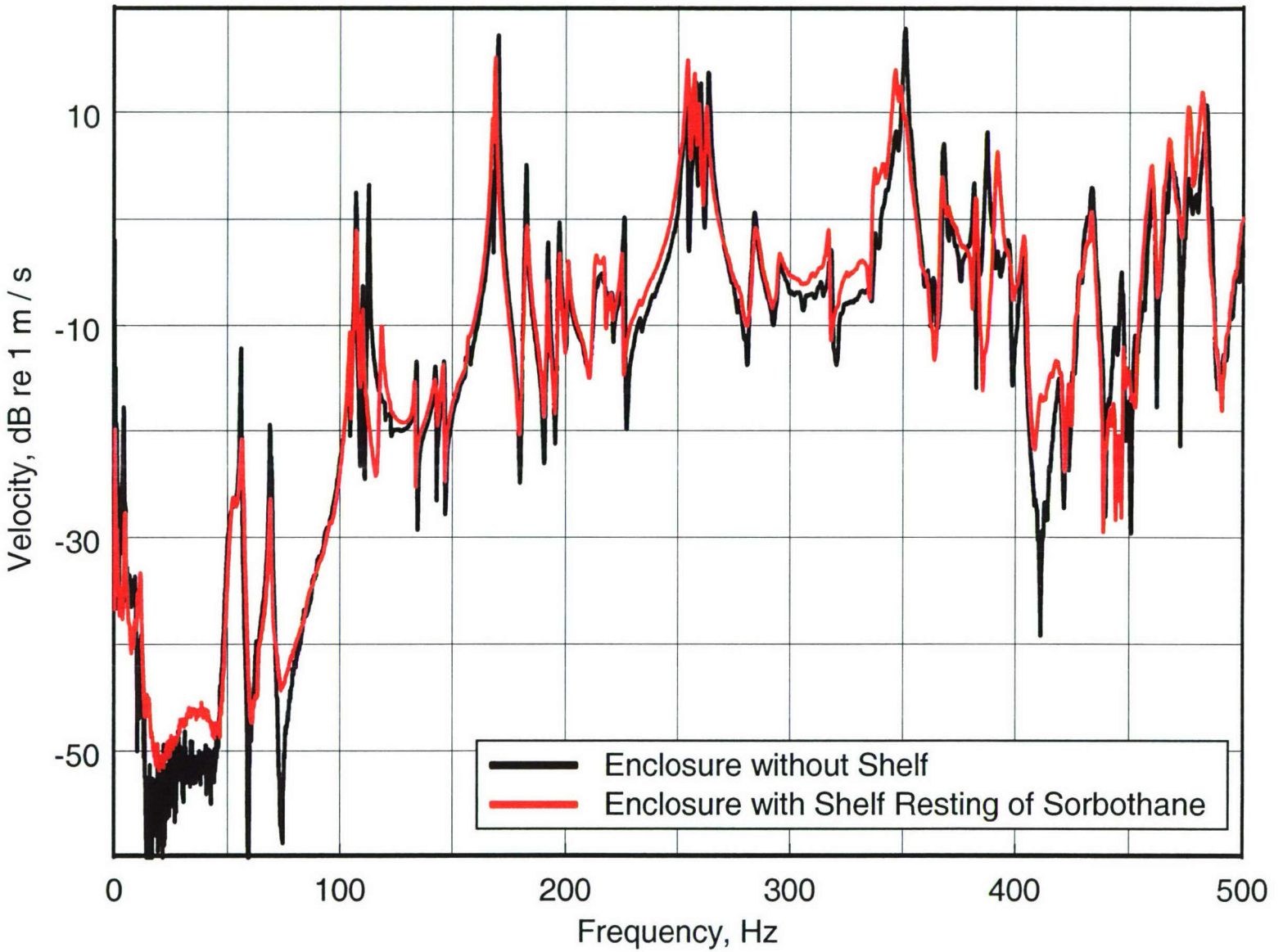

Figure 10. Comparison of the enclosure vibration levels for a drive point on Side A

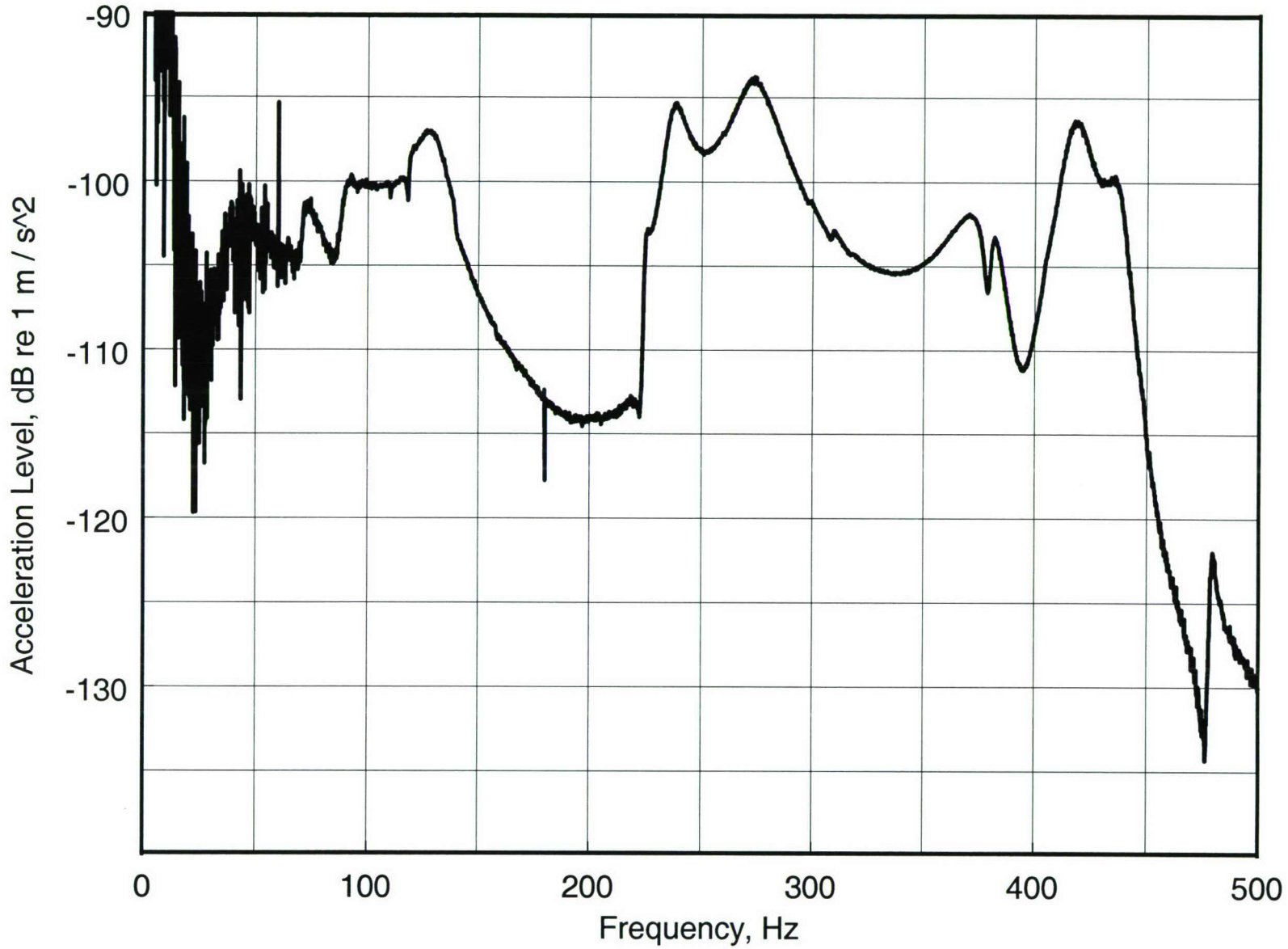

Figure 11. Acceleration levels on the shelf resting on sorbothane for shaker excitation

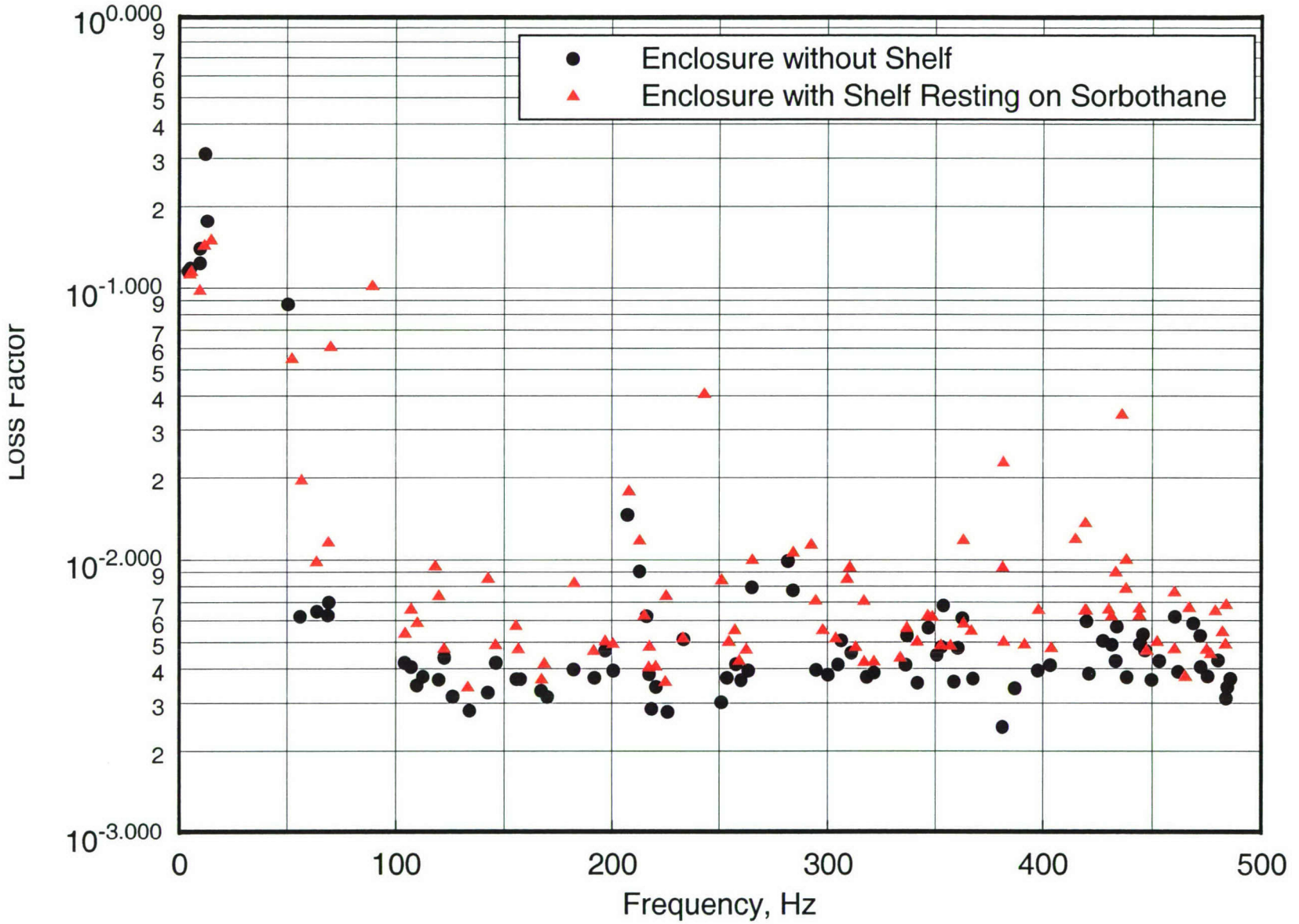

Figure 12. Comparison of the damping loss factors for the enclosure

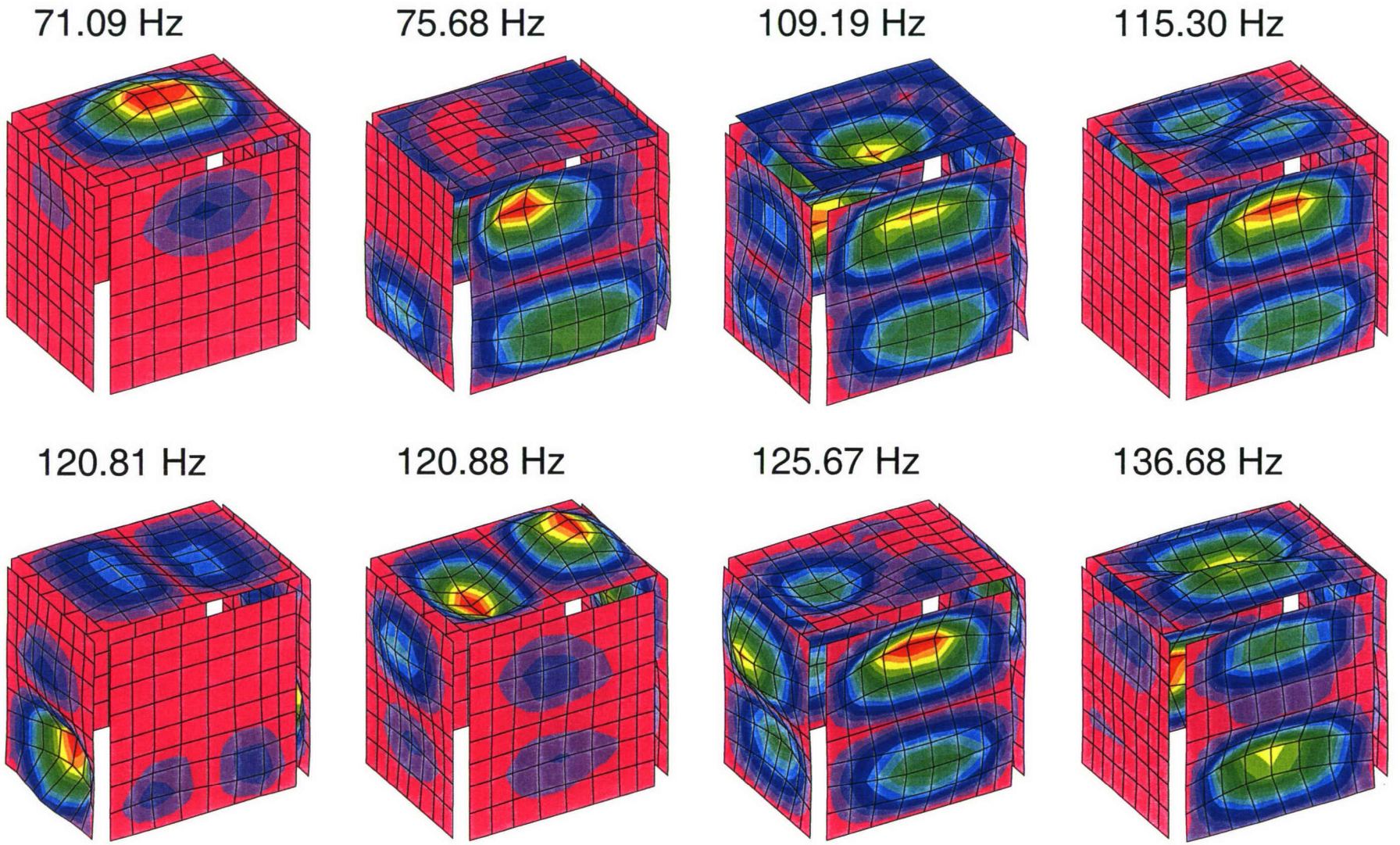

Figure 13. First eight mode shapes with the shelf hinged to the sides

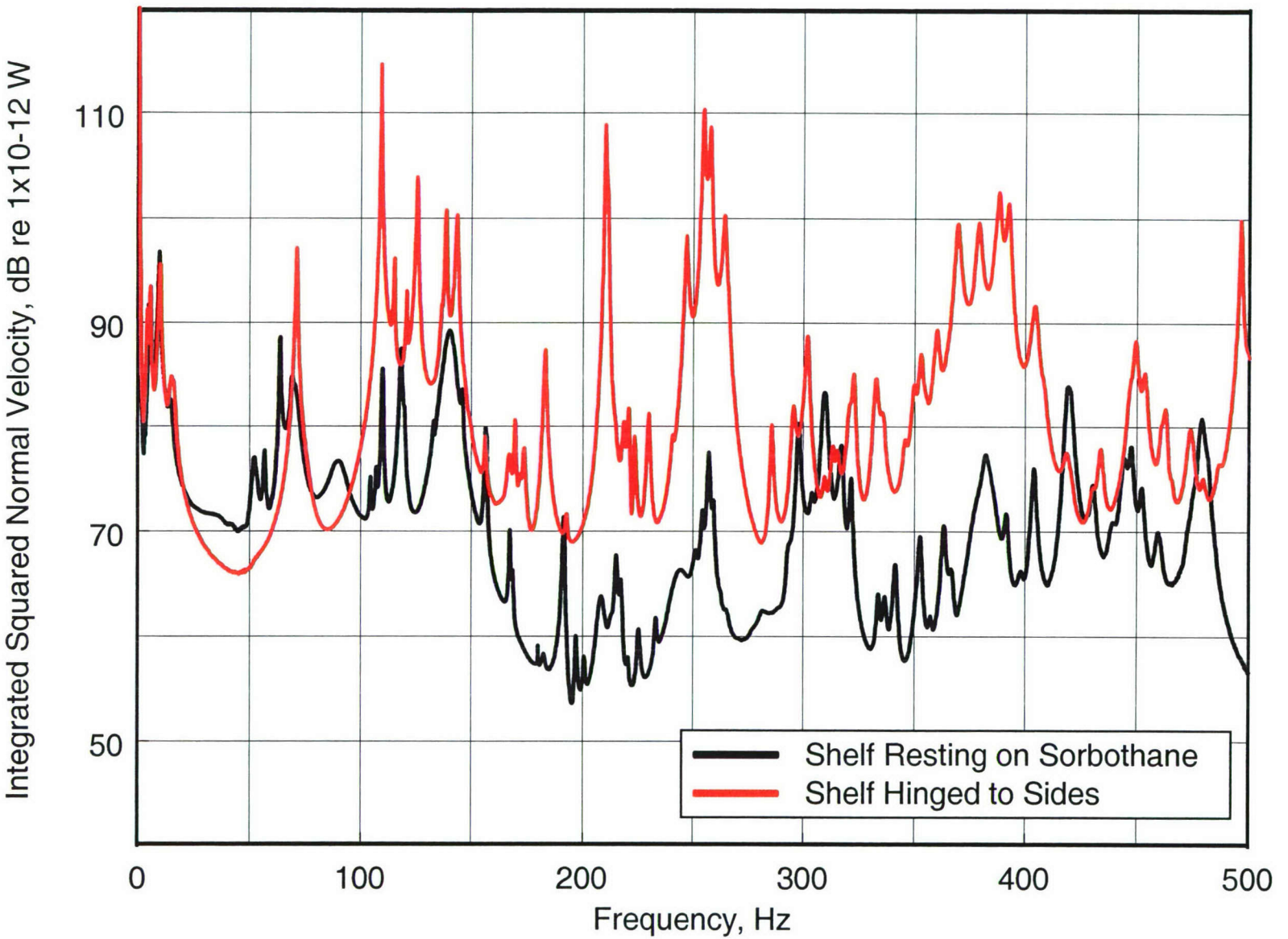

Figure 14. Comparison of the enclosure vibration levels for a drive point on the shelf

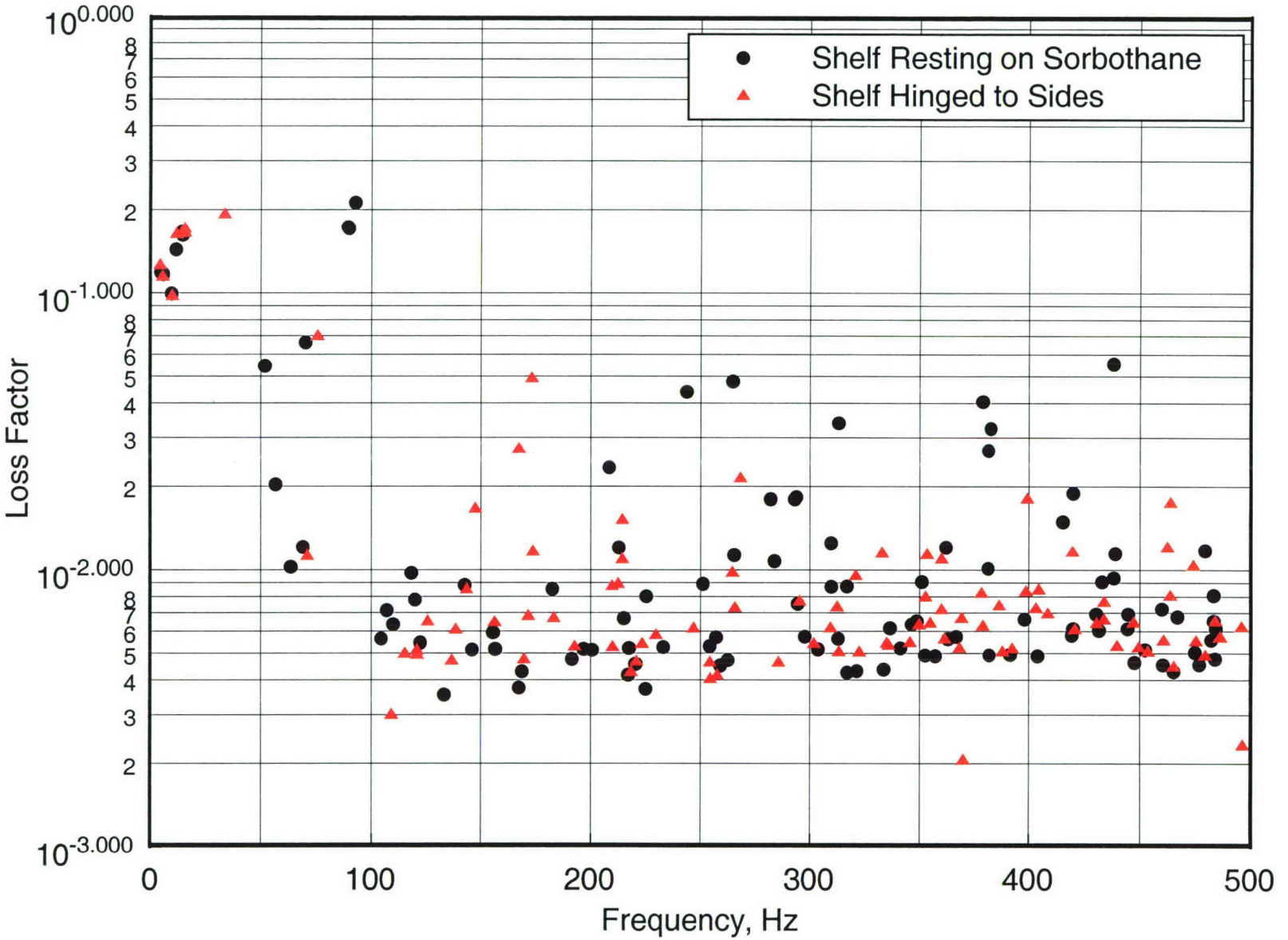

Figure 15. Comparison of the loss factors for the enclosure

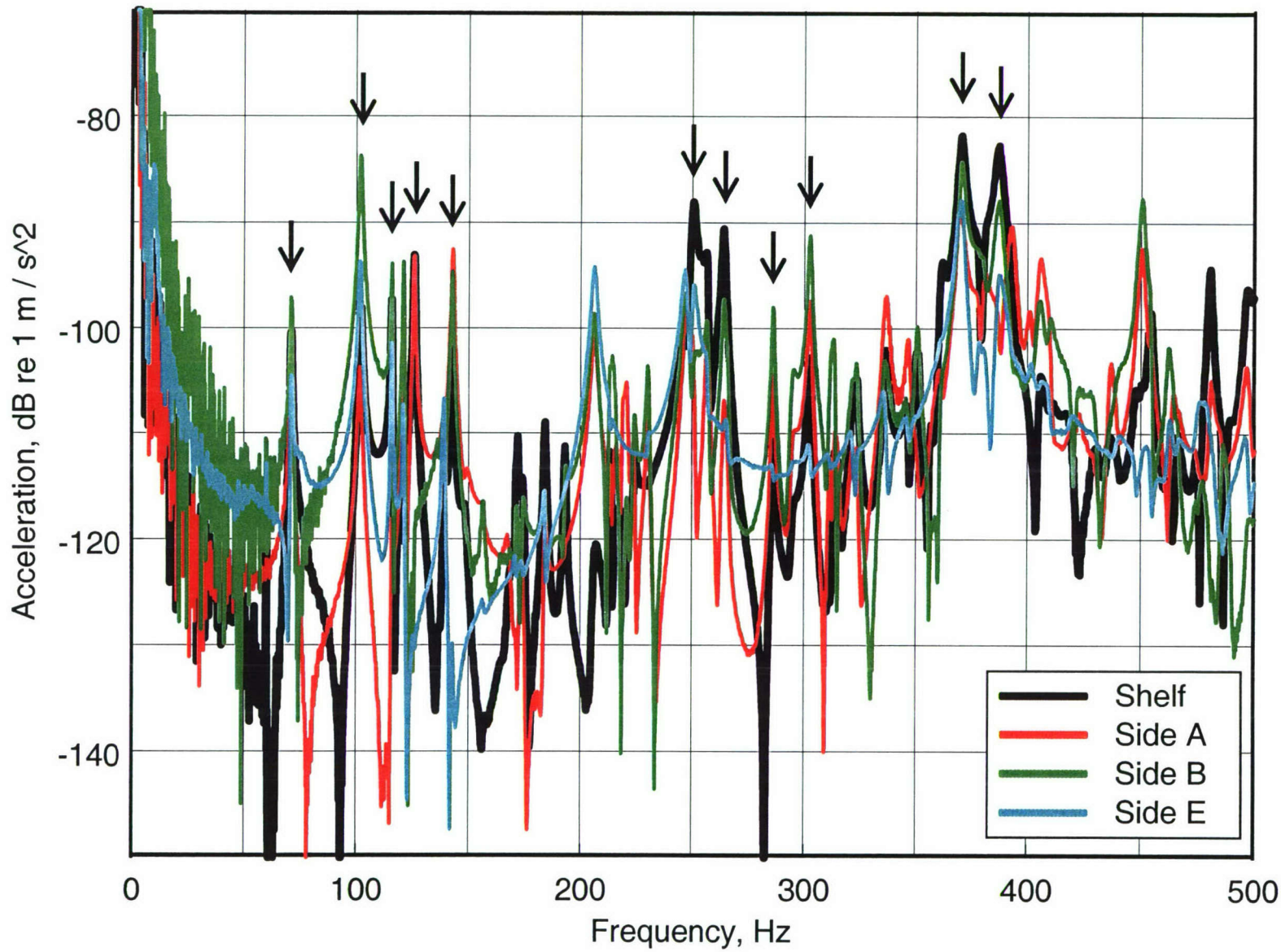

Figure 16. Comparison of the acceleration levels at various locations with the shelf hinged

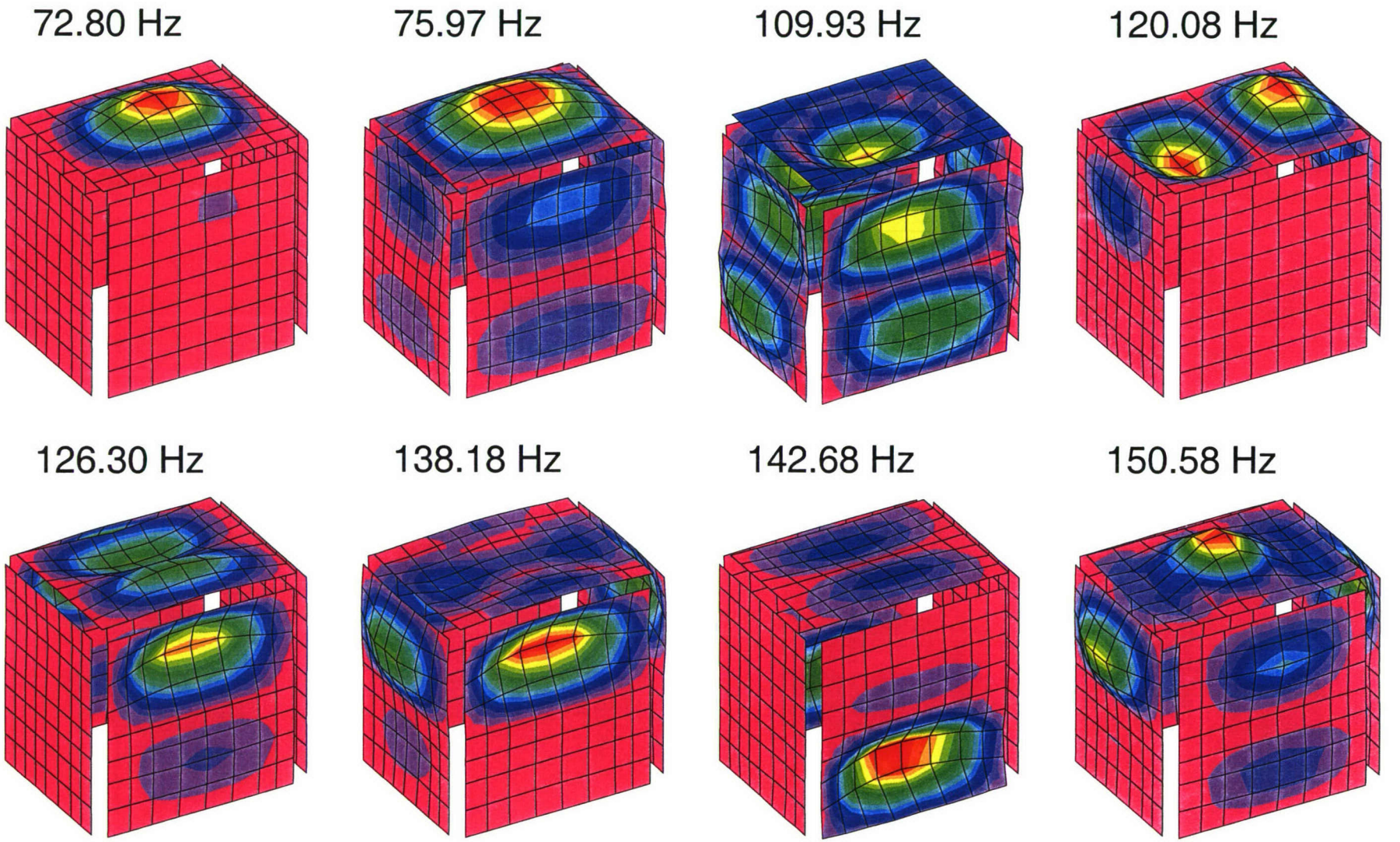

Figure 17. First eight mode shapes with the shelf clamped to the sides

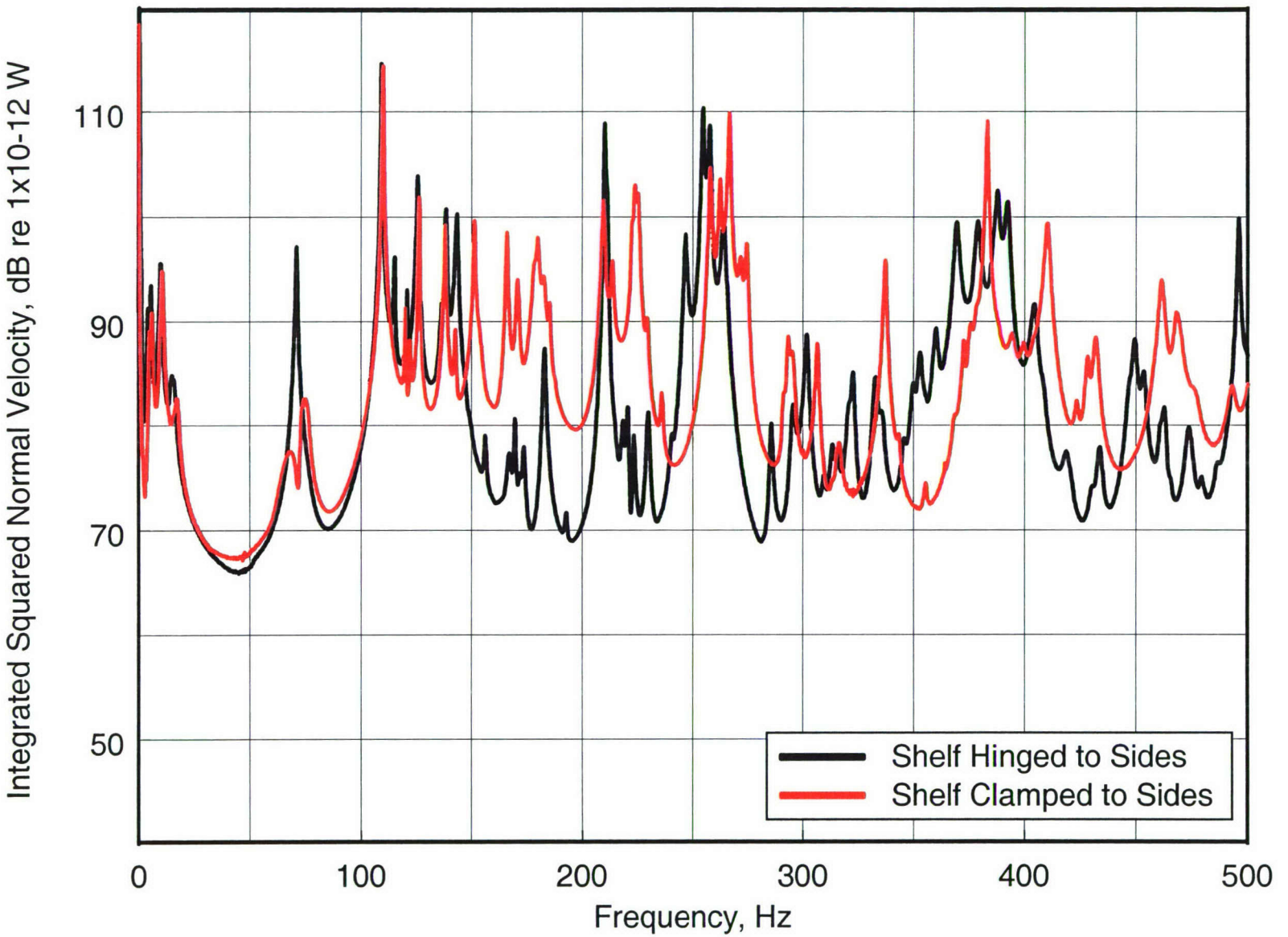

Figure 18. Comparison of the enclosure vibration levels for a drive point on the shelf

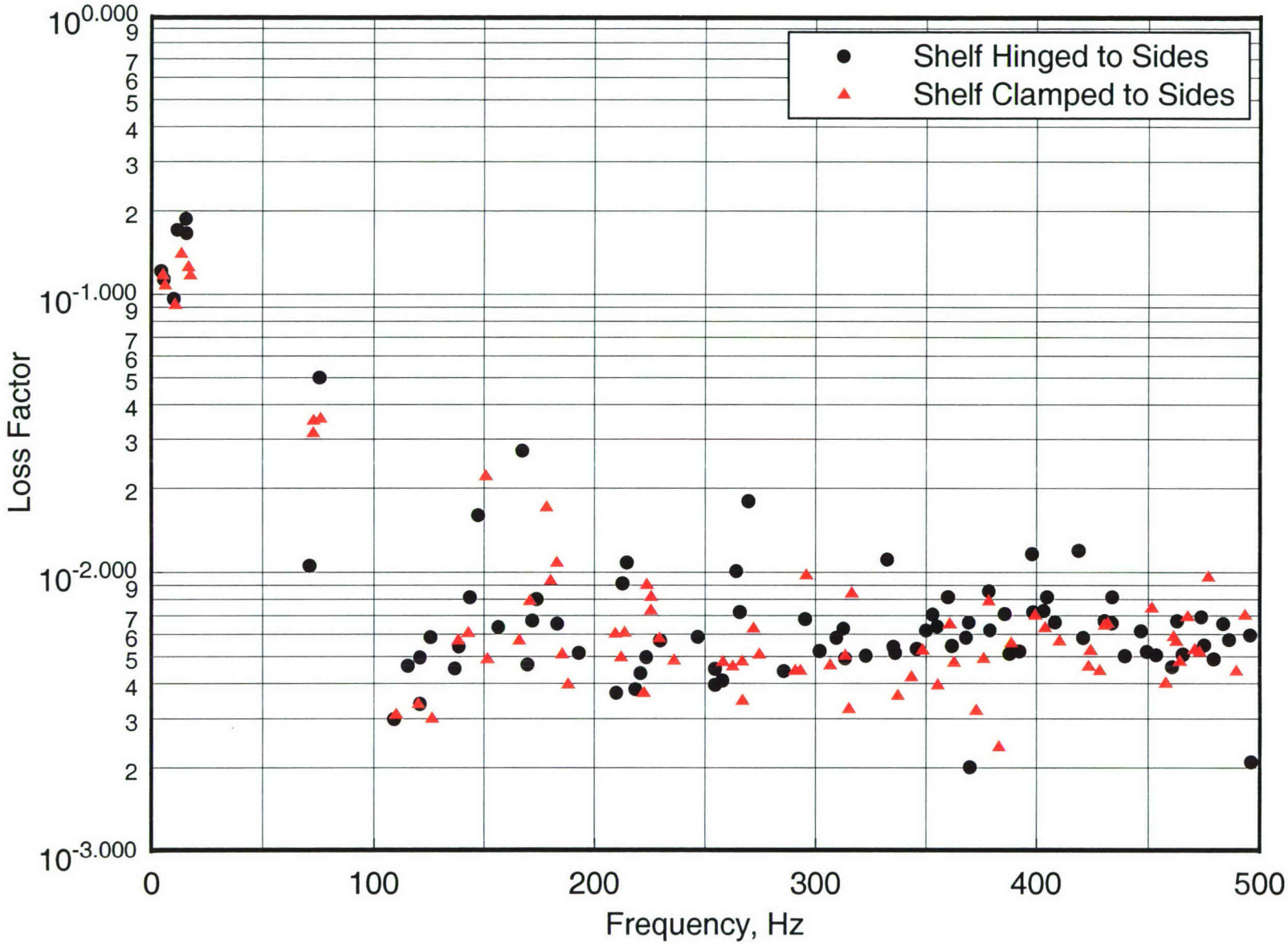

Figure 19. Comparison of the loss factors for the enclosure

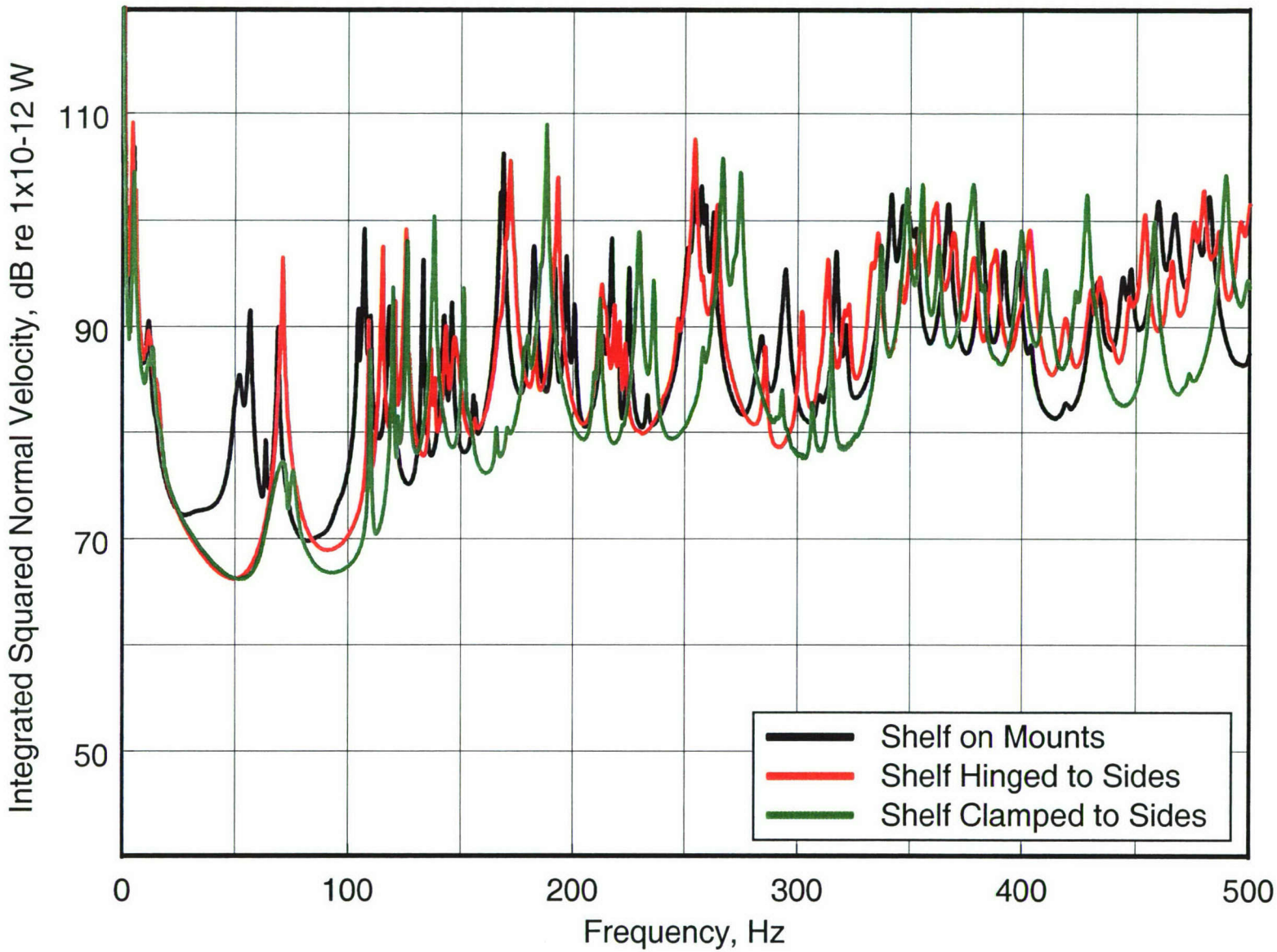

Figure 20. Comparison of the enclosure vibration levels for a drive point on the Side A

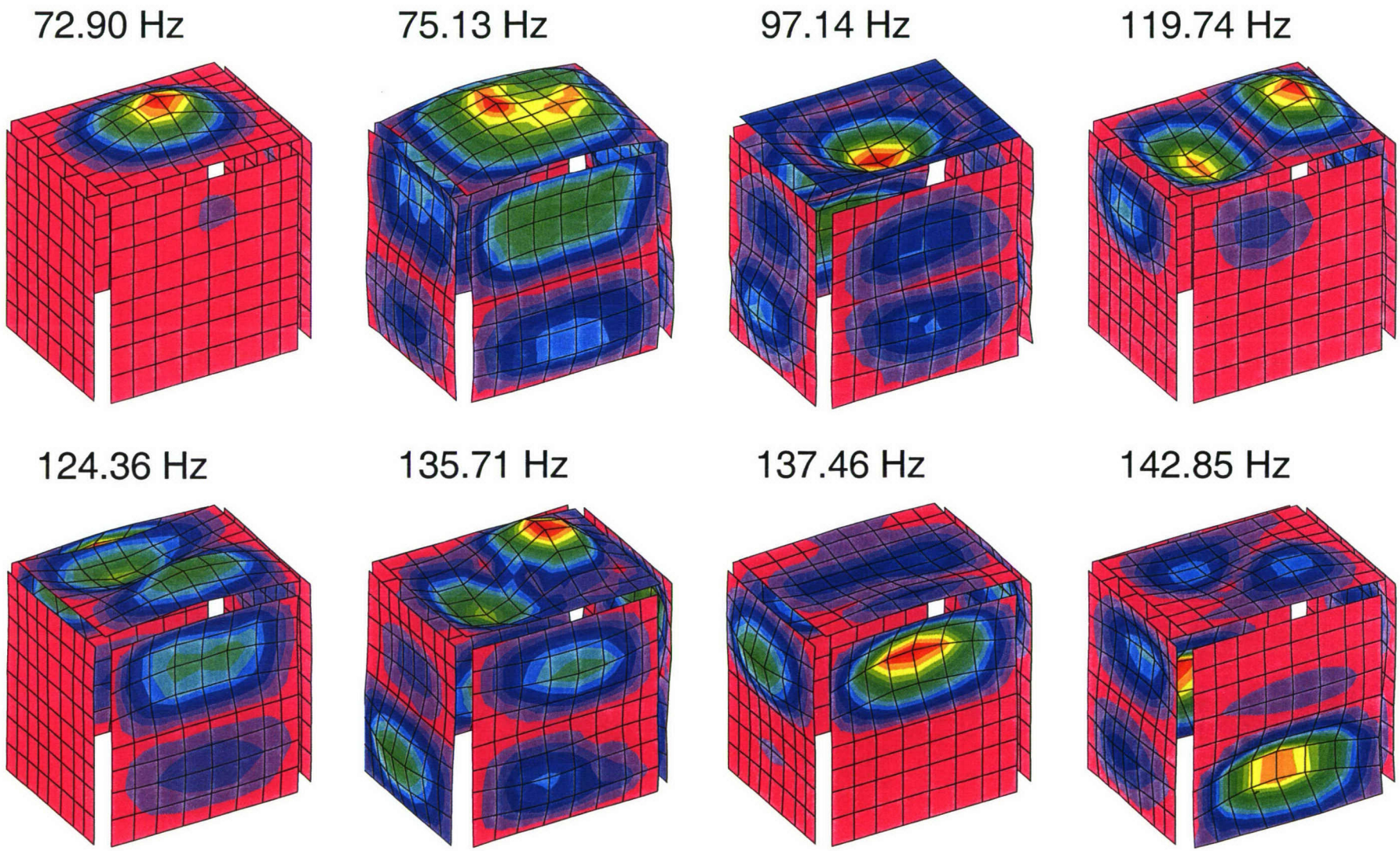

Figure 21. First eight mode shapes with the shelf clamped and with dummy masses

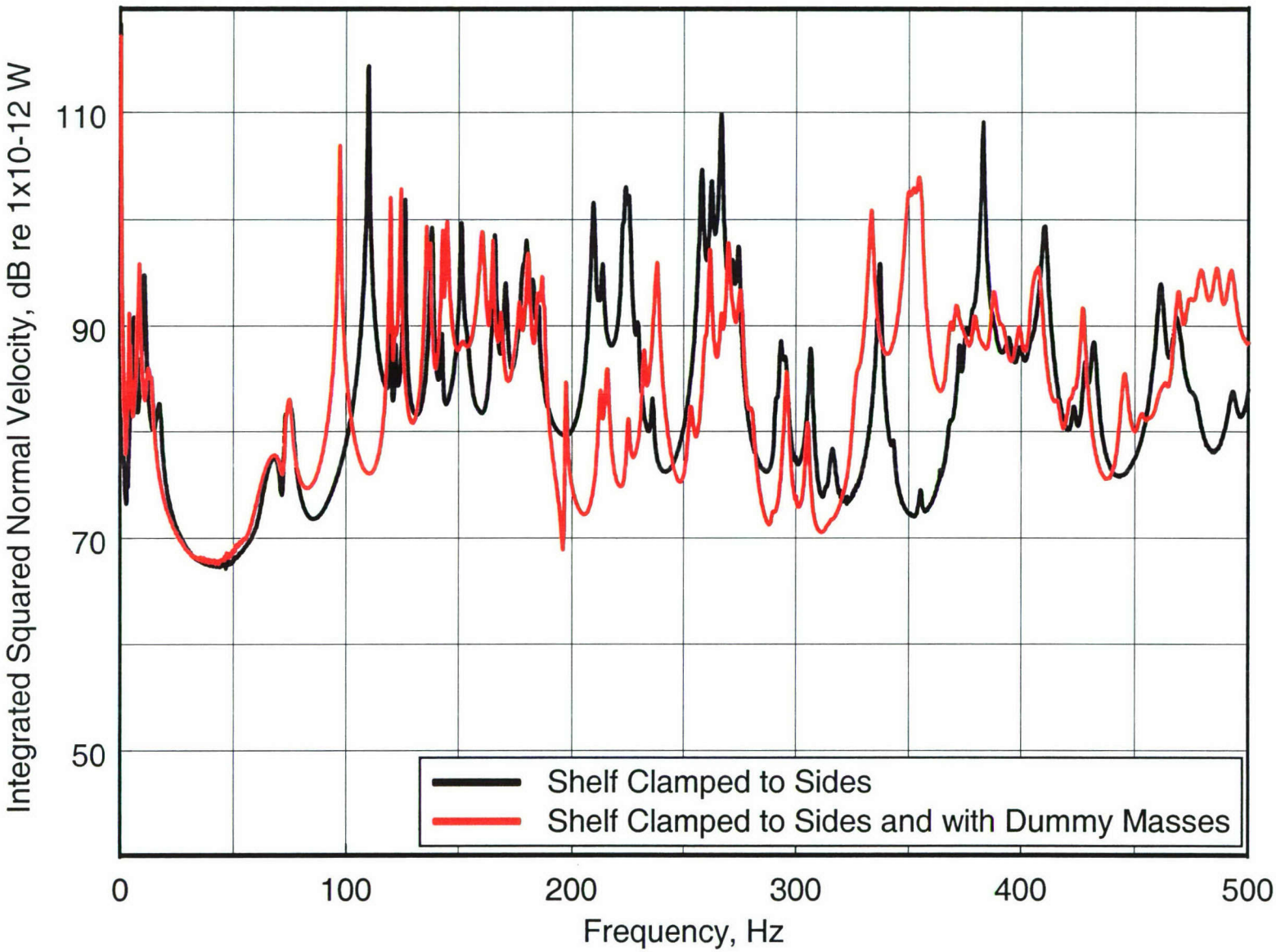

Figure 22. Comparison of the enclosure vibration levels for a drive point on the shelf

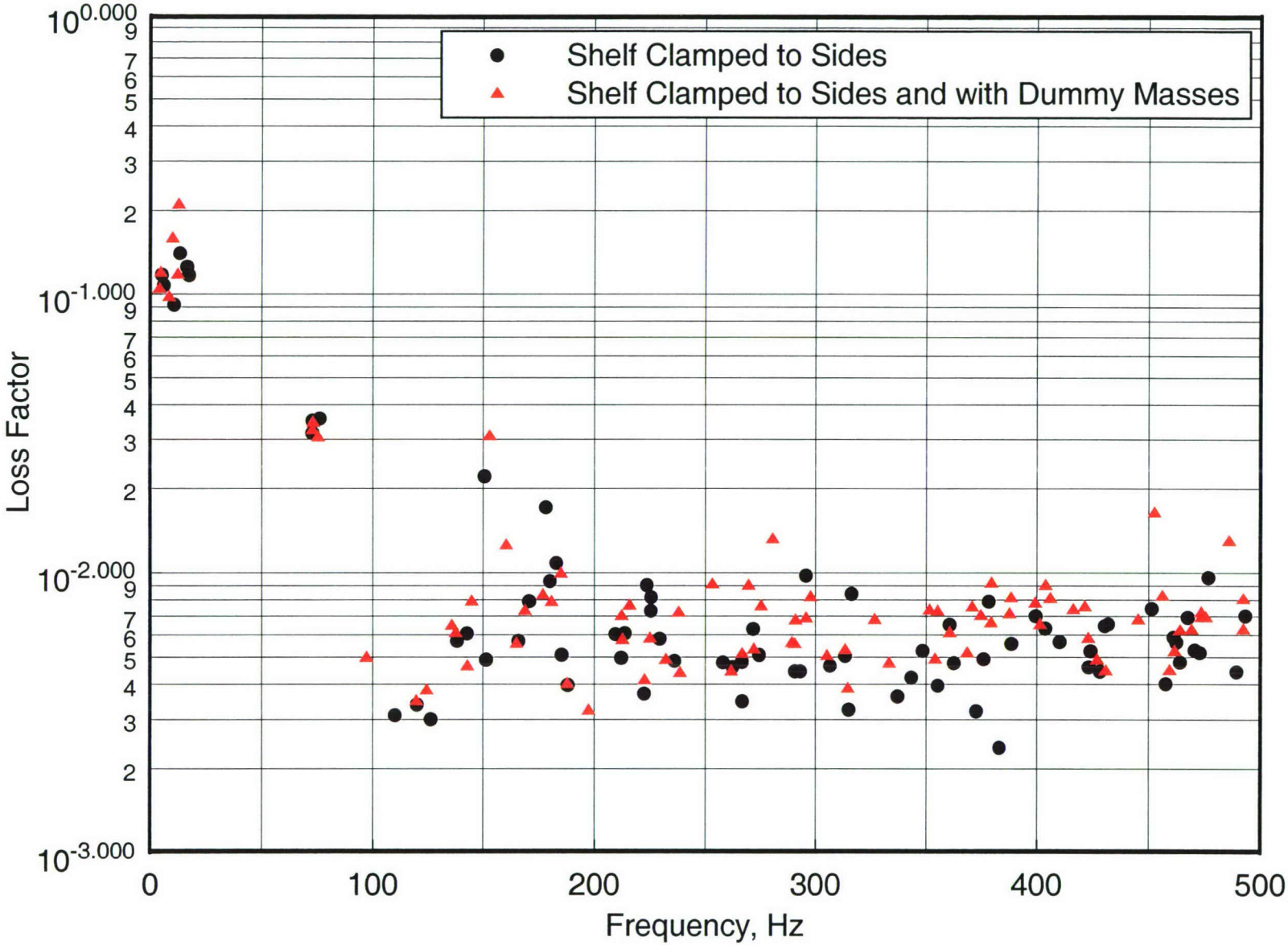

Figure 23. Comparison of the loss factors for the enclosure

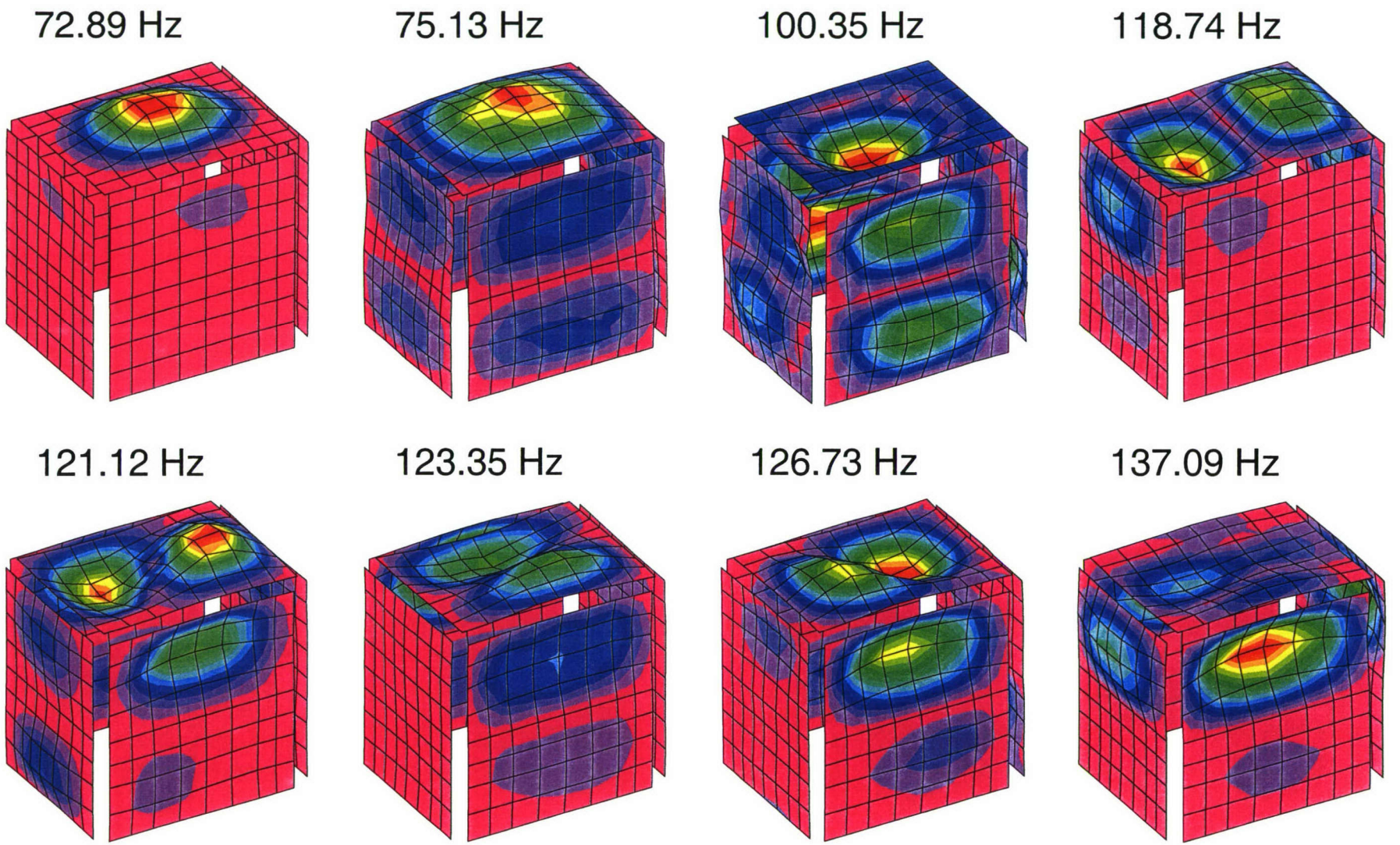

Figure 24. First eight mode shapes with the shelf clamped and with real equipment

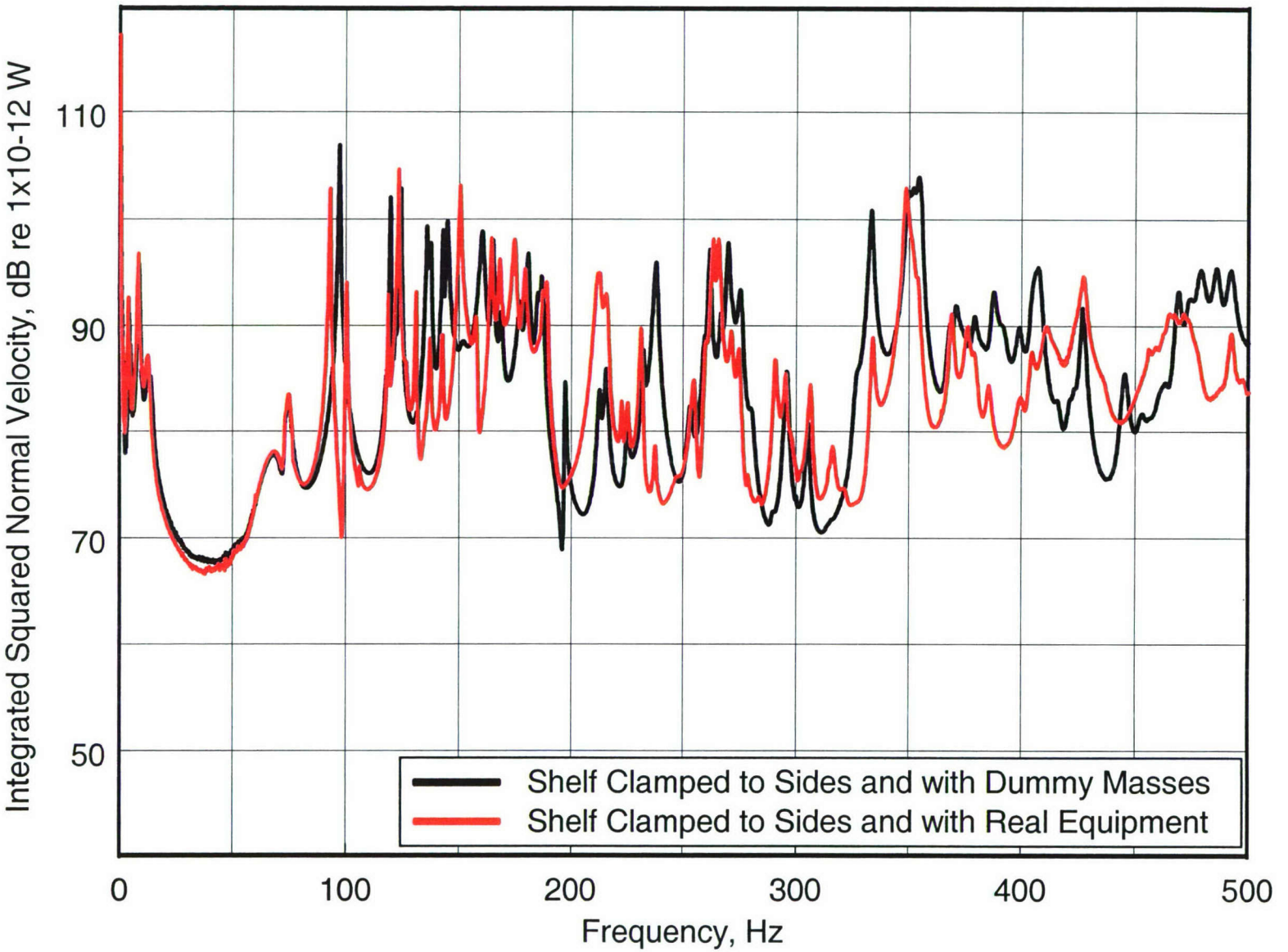

Figure 25. Comparison of the enclosure vibration levels for a drive point on the shelf

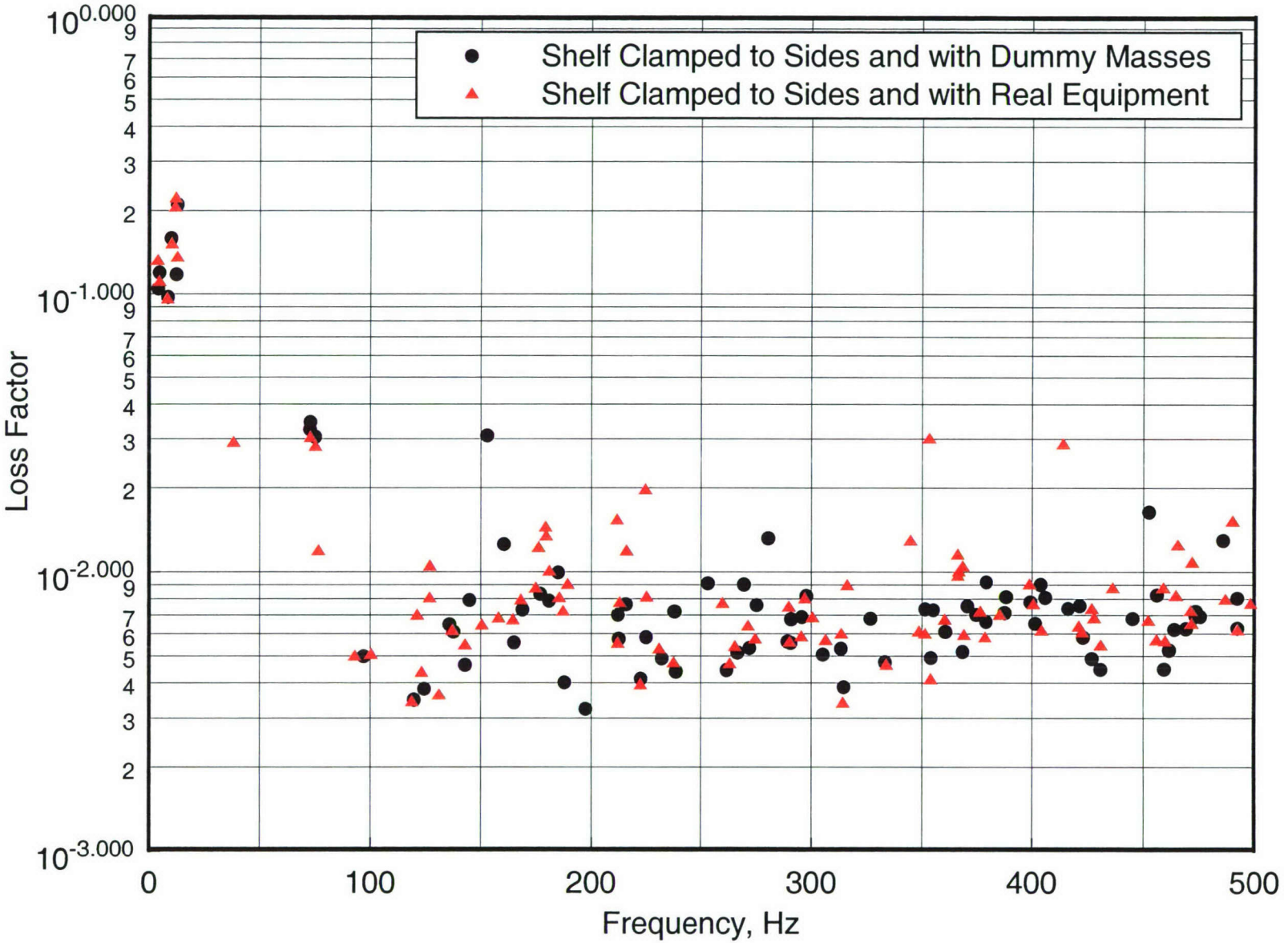

Figure 26. Comparison of the loss factors for the enclosure

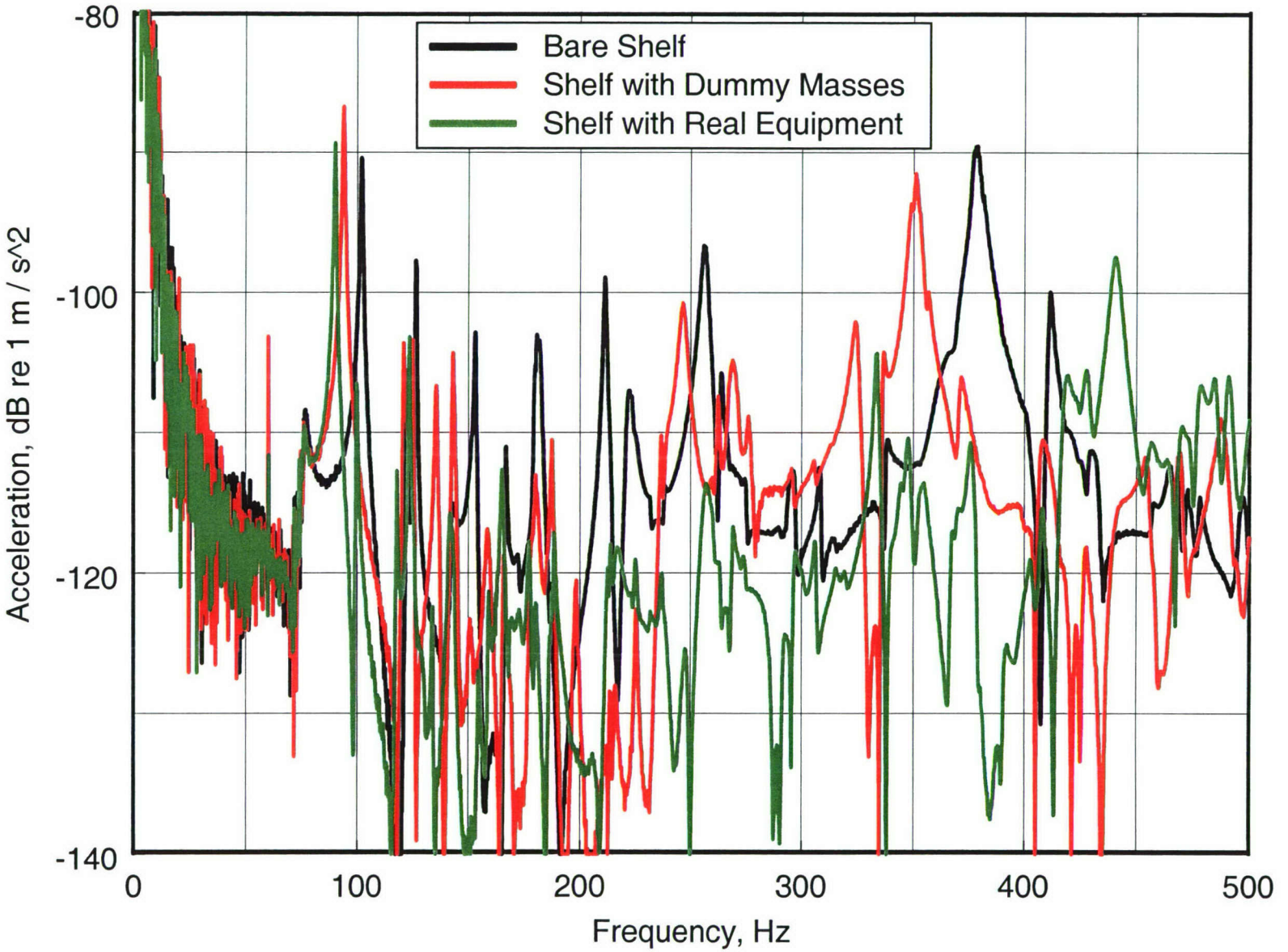

Figure 27. Comparison of drive point acceleration levels for a drive point on the shelf

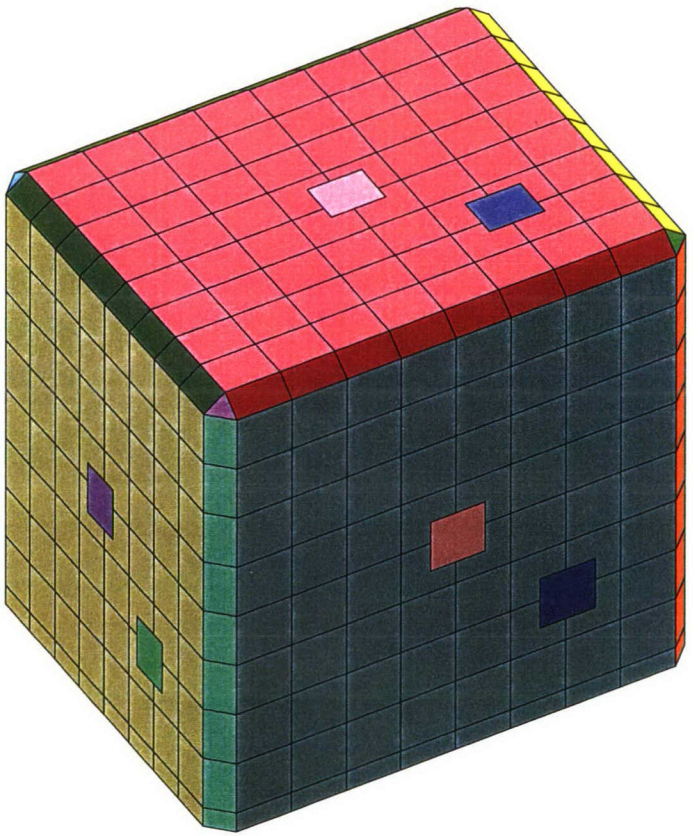

Figure 28. Pressure measurement locations near the enclosure surface

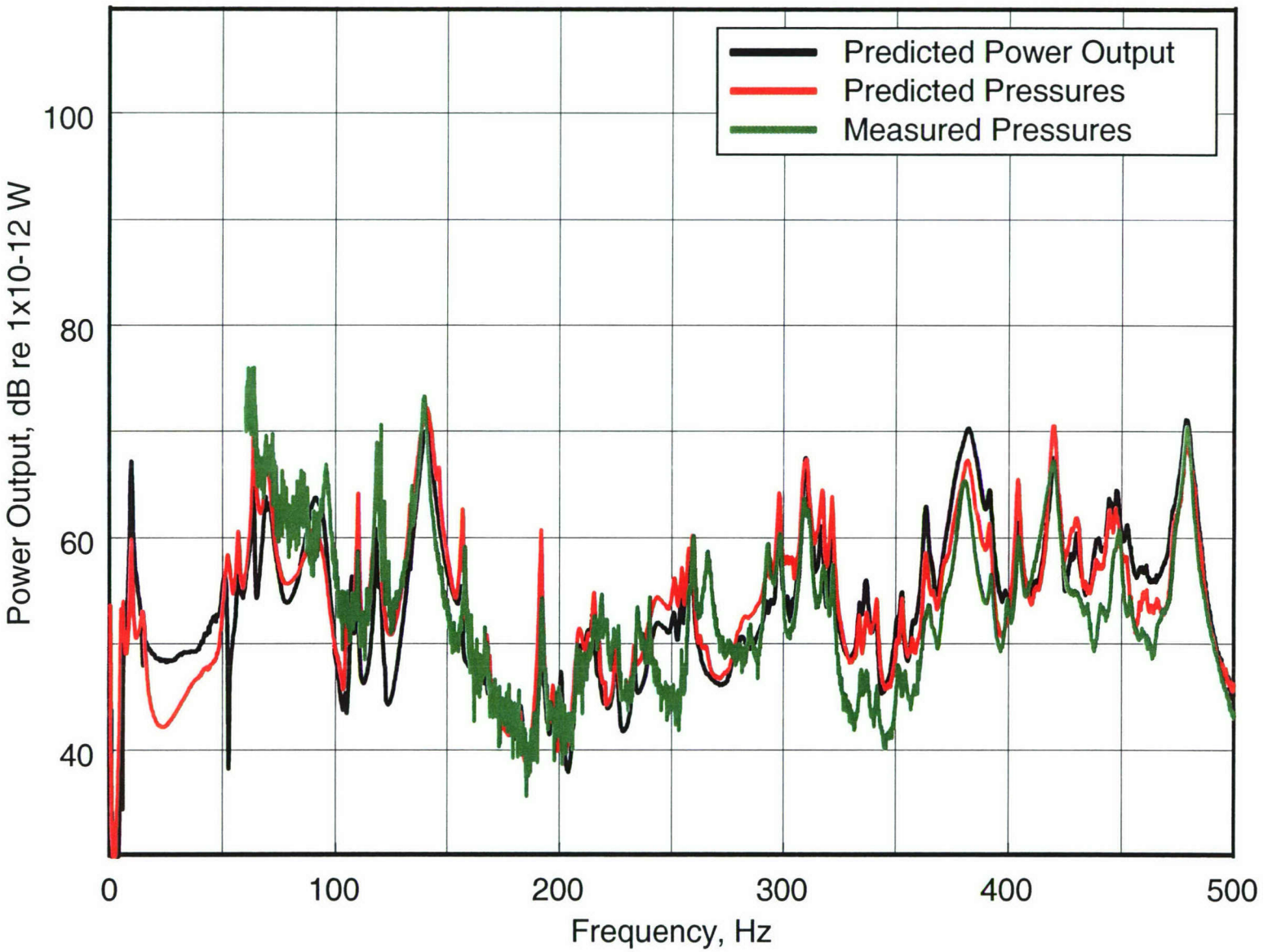

Figure 29. Comparison of the summed pressures with the shelf resting on sorbothane

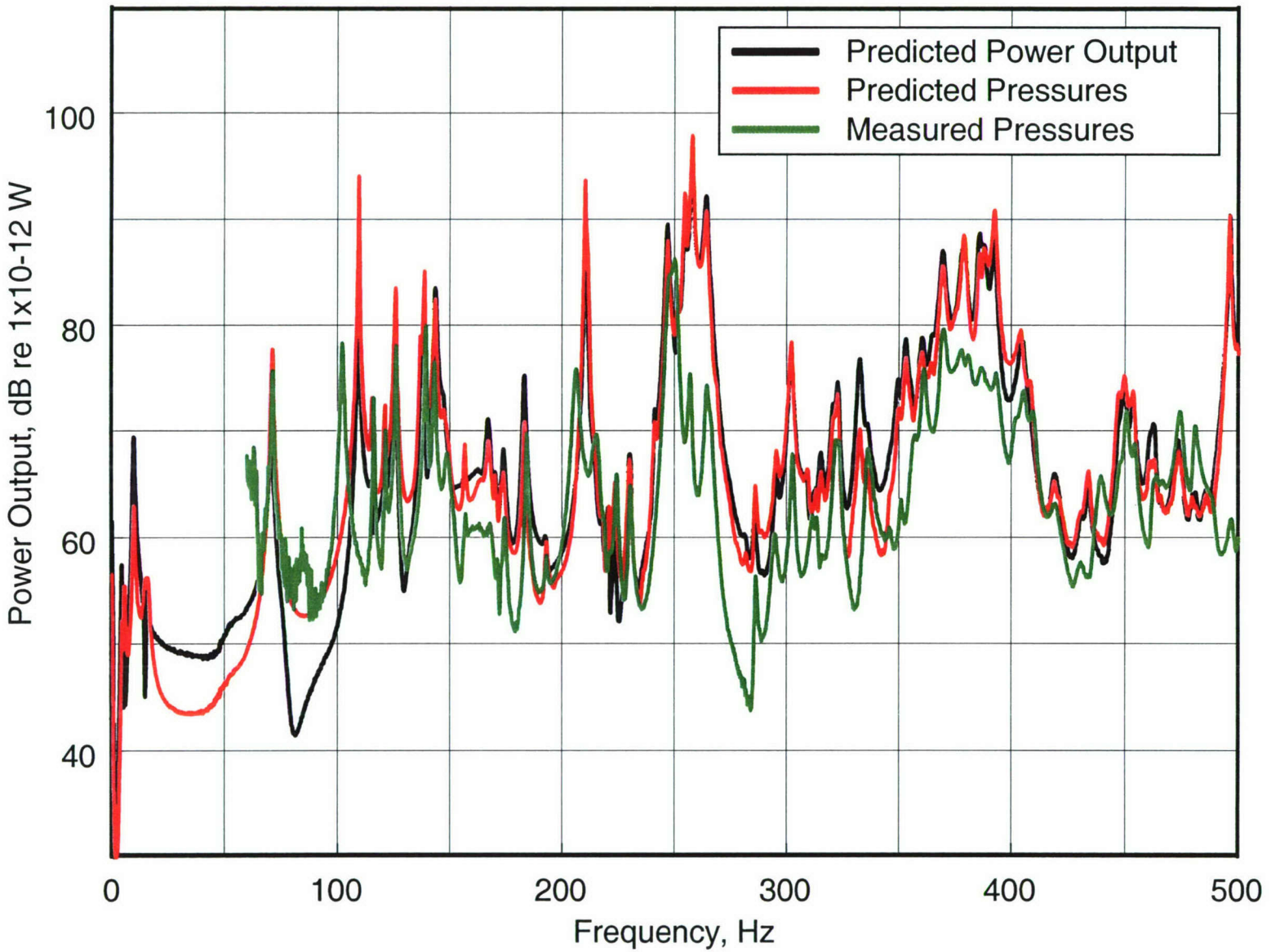

Figure 30. Comparison of the summed pressures with the shelf hinged to the sides

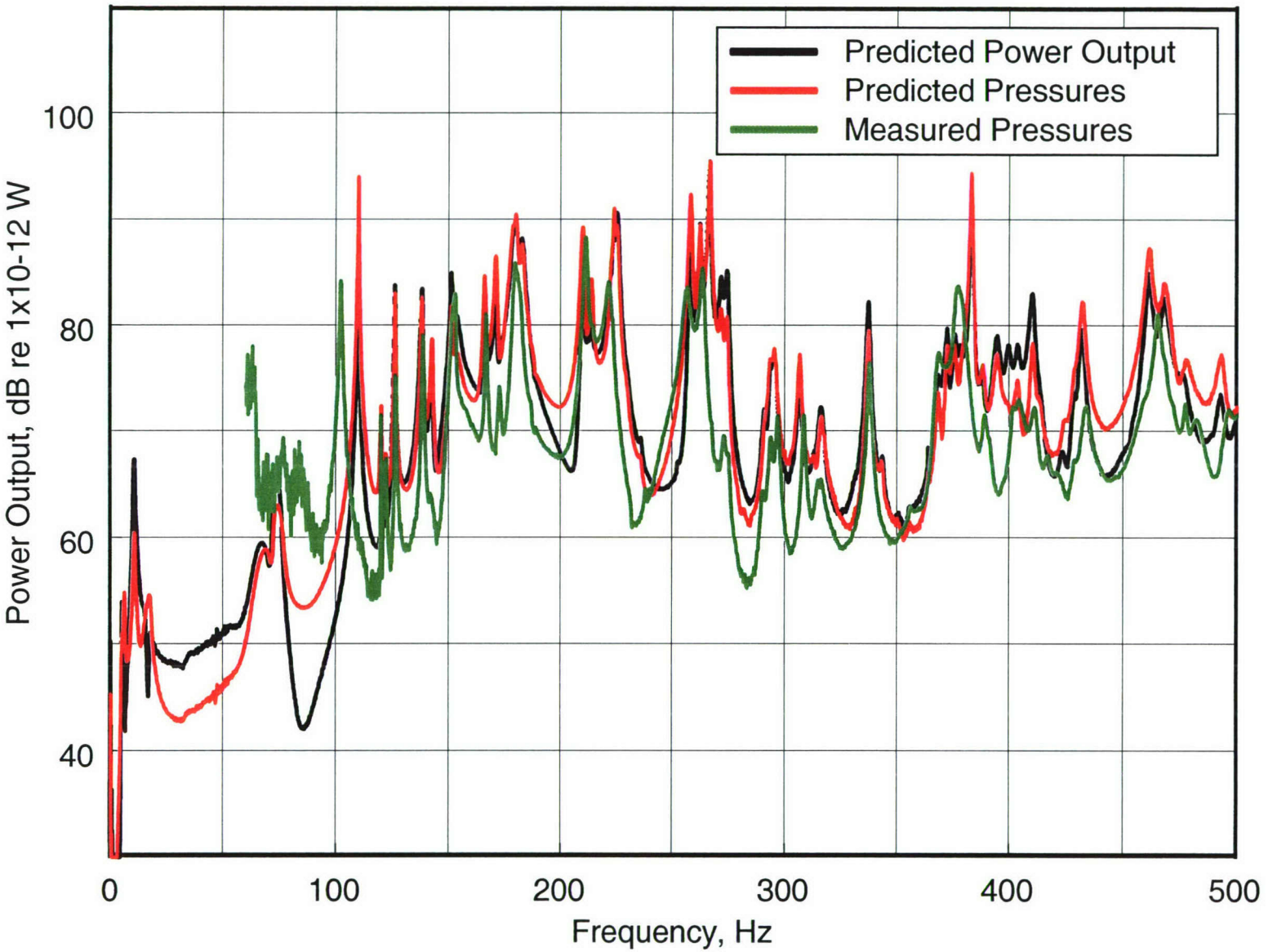

Figure 31. Comparison of the summed pressures with the shelf clamped to the sides

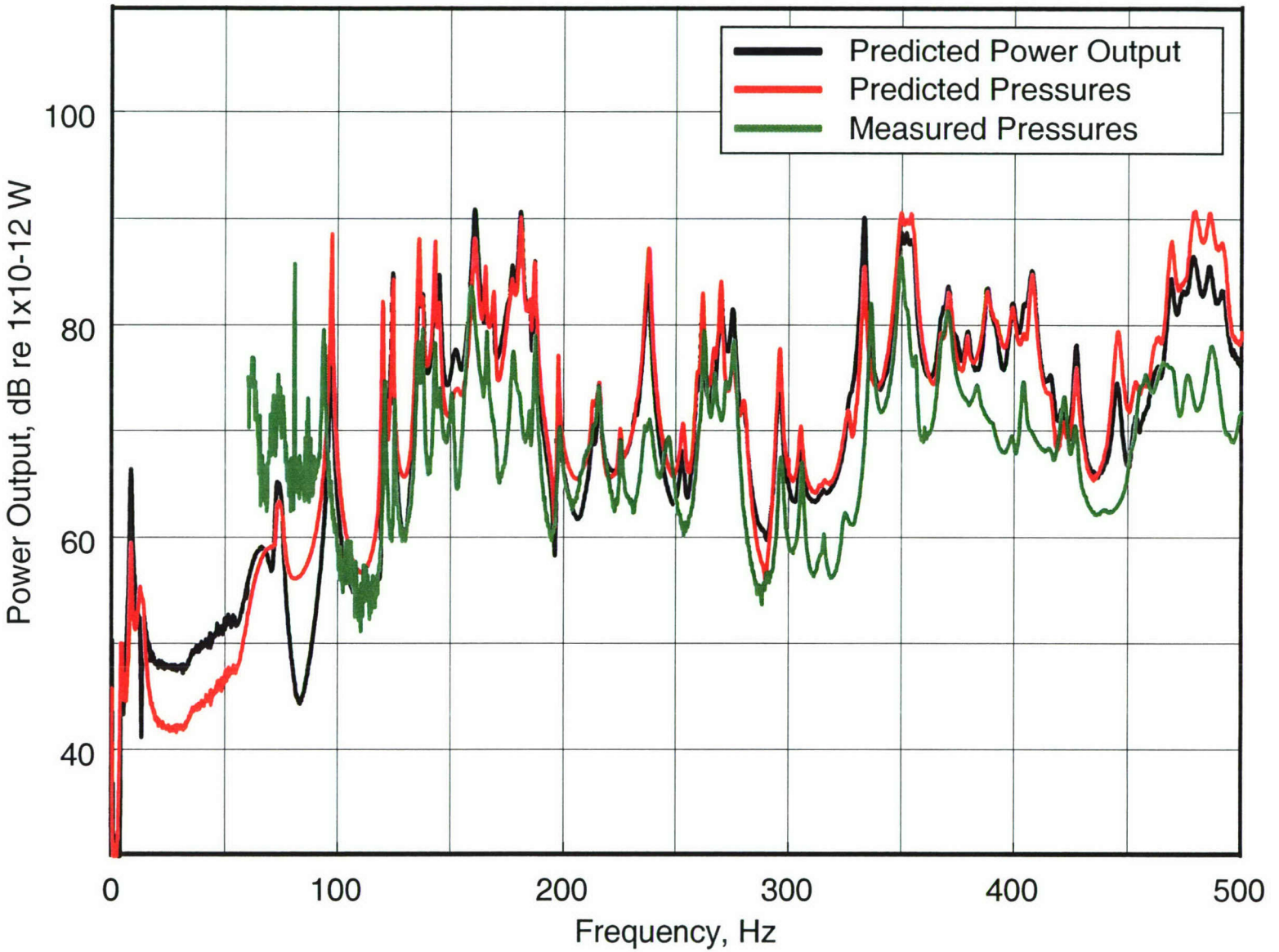

Figure 32. Comparison of the summed pressures with dummy masses on the clamped shelf

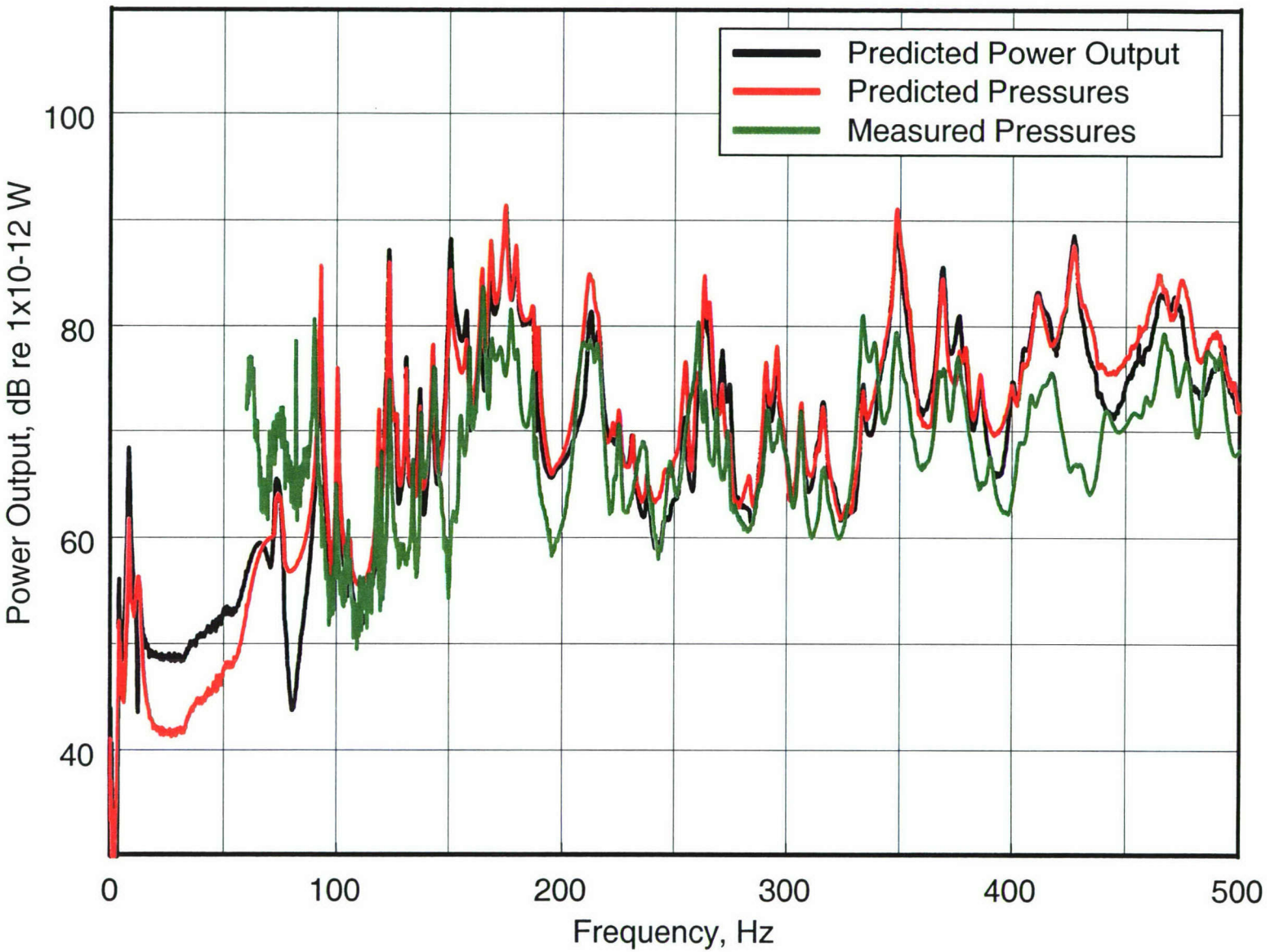

Figure 33. Comparison of the summed pressures with real equipment on the clamped shelf

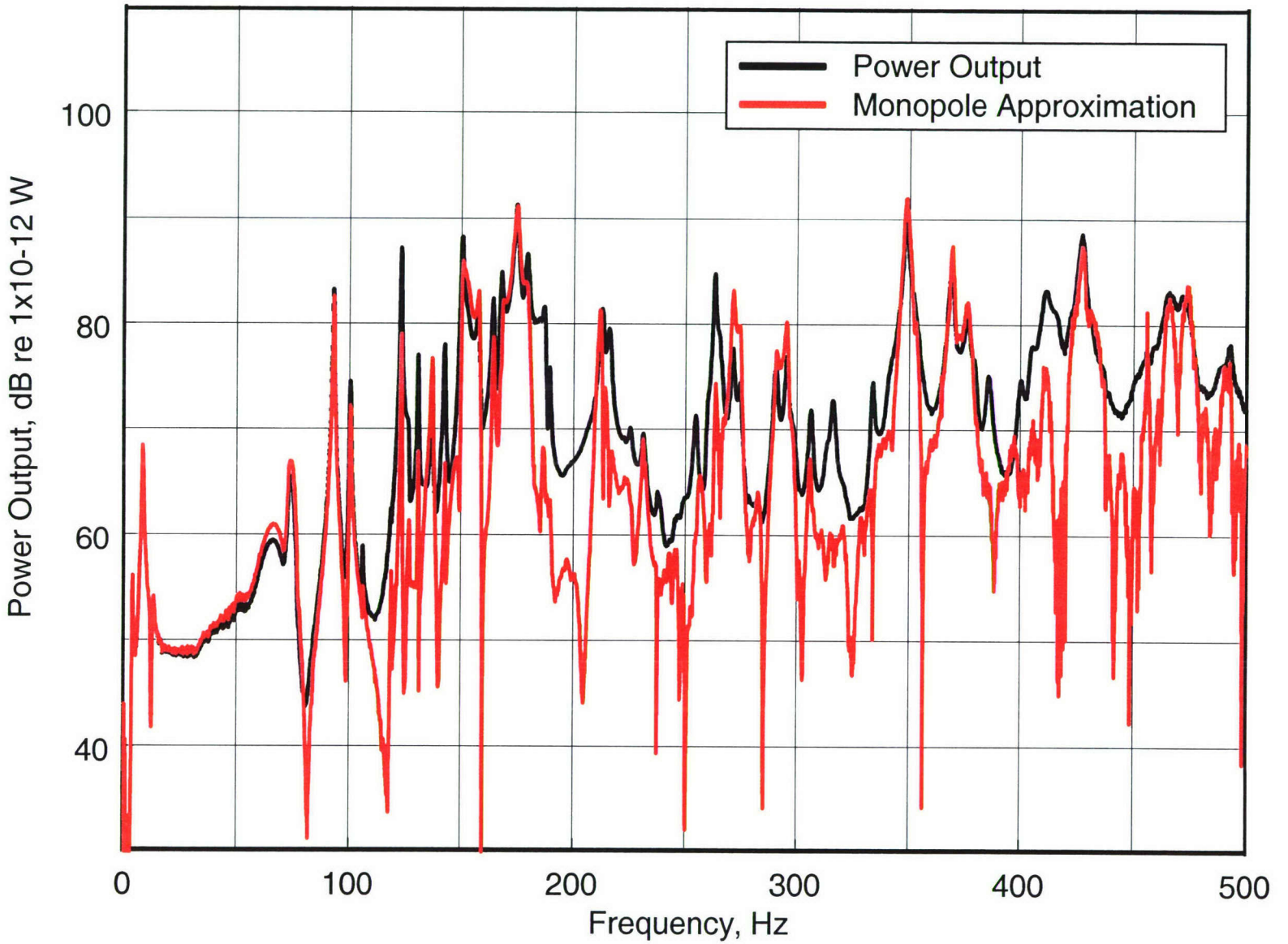

Figure 34. Comparison of the monopole approximation with the actual power output